Arabian Journal of Chemistry (2022) **15**, 103685

King Saud University

Arabian Journal of Chemistry

www.ksu.edu.sa
www.sciencedirect.com

ORIGINAL ARTICLE

Microwave assisted green synthesis of Fe@Au core–shell NPs magnetic to enhance olive oil efficiency on eradication of helicobacter pylori (life preserver)

Najlaa S. Al-Radadi

Department of Chemistry, Faculty of Science, Taibah University, P.O. Box 30002, Al-Madinah Al-Munawarah 14177, Saudi Arabia

Received 9 August 2021; accepted 4 January 2022
Available online 10 January 2022

KEYWORDS

Fe@AuNPs;
Antibiotics;
Vitamin E;
Lauric acid;
Anti-ulcer;
Helicobacter pylori

Abstract Eco friendly and green synthetic approach for the synthesis of metallic nanoparticles gained much importance in the recent era. In the present study, an environmental friendly and plant mediated synthetic approach was used for the synthesis of gold coated iron (Fe@Au) nanoparticles using extract solution of olive oil, licorice root *(Glycyrrhiza glabra)* and coconut oil (OLC). These extracts were acted as a reducing agent during the formation of core–shell nanoparticles that provides long-time stability, lower toxicity and higher permeability to specific target cells. In order to achieve the small sized, regular spherical shaped, and homogeneous nanoparticles optimum conditions were ensured. In fact, the use of microwave irradiation was offered higher reaction rate and better product. The Fe@AuNPs have been characterized by UV–Visible spectroscopy, Energy dispersive X-ray spectroscopy (EDX), X-ray diffraction (XRD), High resolution Transmission electron microscope (HR-TEM), Fourier Transform Infrared Spectroscopy (FT-IR), high-performance liquid chromatography (HPLC), High angle annular dark-field scanning transmission electron microscopy (HAADF-STEM), Particle-Size Distribution (PSD), and Magnetic hysteresis loops. The synthesized gold coated iron nanoparticles showed significant antioxidant potential with maximum inhibition rates, the biosynthesized nanoparticles were also found effective against *Helicobacter pylori* (*H. pylori*) and ulcer.

1. Introduction

Nanoscience appeared in 1990 (Al-Radadi, 2018), a science concerned with the investigation of the possibilities of modifying the material at the nano-scale in order to generate new materials or sophisticated gadgets to serve human needs in a variety of disciplines. The size of nanoparticles spans from 1

E-mail address: nsa@taibahu.edu.sa
Peer review under responsibility of King Saud University.

Production and hosting by Elsevier

https://doi.org/10.1016/j.arabjc.2022.103685
1878-5352

to 100 nm, with 1 nm equaling 10^{-9} m (Ionescu, 2016; Khan et al., 2019a; Sathiyanarayanan et al., 2017; Thakkar et al., 2010), There are two approaches for creating nanomaterials in nanomaterials technology: bottom-up and top-down (Al-Radadi, 2019; Chen & Liu, 2018; Fathi-Achachelouei et al., 2019; Rudramurthy & Swamy, 2018; Serhan et al., 2019) nanoparticles offers a wide range of uses in cancer treatment without needing surgery, such as medication administration and release, as well as in maintaining blood sugar levels low, and in biotechnology. (Ghormade et al., 2011; Lombardo et al., 2019; Martin, 2019), chemistry (Alam et al., 2016; Martínez-Prieto & Chaudret (2018)), electronics (Li et al., 2018; Tavakoli et al., 2018), agriculture (Kumar et al., 2019a) and so on. These are not the only uses for NPs; there are others, such as smart materials and biosensors (Wang et al., 2018; Chen et al., 2019b). The use of chemicals and organic solvents as reducing and capping agents in the synthesis of metallic NPs is an effective and successful yet but hazardous procedure (Singera et al., 2019), As a result, plant-mediated synthesis is favored over chemical approaches since researchers have chose a process that is safe, ecologically friendly, and has no side effects, which is the Green synthesis of nanoparticles and its main applications in diverse industries (Sharma and Tripathi, 2021; Anjana et al., 2019; Khan et al., 2019b). Plant extracts of various varieties can also be employed, including plant components such as leaves, stems, roots, flowers, fruit, and vegetable and fruit waste. (Al-Radadi & Adam, 2020; Menazea et al., 2021; Kumar et al., 2021; Al-Radadi, 2021a) due to its unique and novel catalytic properties (Ahmed et al., 2016; Khan et al., 2017; Narayan et al., 2019; Rao & Paria, 2015). The characteristics of the metals utilized in the creation of nanoparticles altered dramatically at the nanoscale, and hence their relevance is recognized in biological and electrical applications. (Abdullah et al., 2022; Devi et al., 2019; Karthik et al., 2016; Paciotti et al., 2004; Rizvi & Saleh, 2018). Au-NPs are far different from bulk gold in physical and chemical properties (Nafisi & Maibach, 2017; Vijayan et al., 2018; Zhu et al., 2019). Gold nanoparticles are one of the most prevalent nanometals, and they have received a lot of attention from scientists in recent years due to their wide range of possible uses in the medical field (Hosny & Fawzy, 2021; Chen et al., 2021; Muniyappan et al., 2021; Qin et al., 2018). Iron nanoparticles are active, and rapidly oxidized to form free iron ions and widely used in medical applications (Obaidat et al., 2014; Rudakov et al., 2019; Rümenapp et al., 2012). Magnetic nanoparticles made of magnetite (Fe_3O_4) or maghemite (y-Fe_2O_3) have received much research due to their vast biological uses. Each medical application necessitates materials with distinct magnetic properties, magnetic properties, and particle shape. Obviously, all materials utilized in these applications must be non-toxic. Many different biological ligands have been functionalized into superparamagnetic iron oxide nanoparticles for interaction with human cancer cells. (Hien Pham et al., 2008; Hassan & Mahmood, 2019). Magnetic particles have characteristics that are not seen in other materials that has been utilized in medical applications. Among metal nanoparticles, hybrid or bimetallic NPs have attractive magnetic and core shell features, which improve their biological potential. (Zaleska-Medynska et al., 2016; Faisal Shah et al., 2021). When the Fe—Au core–shell nanoparticles are smaller than 128 nm in size, they become superparamagnetic, preventing self-agglomeration, and their magnetic behavior can only be confirmed when they are exposed to magnetic flux. (Ban et al., 2005; Padma et al., 2014; Zare et al., 217); Mohammadi et al., 2021; Gawande et al., 2015).

Helicobacter pylori (H. pylori), The World Health Organization has categorised a spiral-shaped Gram-negative bacteria as a class I carcinogen and identified it as the causal agent for peptic ulcers, duodenal ulcers, gastritis, mucosa-associated lymphoid tissue lymphomas, and gastric cancer. A link between *H. pylori* infection and functional dyspepsia (FD) has also been shown in a subgroup of affected patients. (Chen et al., 2019a; Koletzko et al., 2019; Aminde et al., 2019; Melese et al., 2019). *H. pylori* is a human-specific pathogen with a strong preference for the mucosa of the stomach. Around half of the world's population is infected with this bacterium (Leja et al., 2016; Wang et al., 2019; Zamani et al., 2018; Verma et al., 2016; Onifade & Bakare, 2019; Ofori et al., 2019; Isaeva & Isaeva, 2020). *H. pylori* may colonies and attach to the stomach epithelium by breaking down urea and producing cell-toxic ammonia. The subsequent pH increase neutralizes stomach acidity, allowing the bacteria to safely pass the mucus layer to the epithelial surface. (Fagoonee & Pellicano, 2019; Farhadkhani et al., 2019; Lakhiar et al., 2018; Etik et al., 2019). Triple therapy consisting of a proton pump inhibitor, clarithromycin and amoxicillin or metronidazole for the treatment of *H. pylori* infection (Murali et al.,2014; Salmanroghani et al., 2018; Collares-Pelizaro et al., 2017; Benites et al., 2018; Modolo et al., 2015). The Pan-Drug Resistant PDR, *H. pylori* remains an intractable challenge in public health worldwide and this pathogenicity is mainly due to the presence of a cytotoxin-associated gene A (CagA) and vacuolating cytotoxin A (VacA) (El-Shouny et al., 2020). Plant extracts, on the other hand, include a varied array of secondary metabolites that might potentially be employed to battle *H. pylori* infections. State-of-the-art studies focused on the potential of plant natural products (available in extracts or as pure compounds) as therapeutic urease inhibitors. (Abou Baker, 2020; Williams, 2011; Díaz-Gómez et al., 2013). The current knowledge on alleviating *H. pylori* infections through the use of some commonly known natural products: bench to bedside such as Syzygium aromaticum, chinese tea, green tea (catechin), matcha tea, Casearia sylvestris leaf, propolis, bulgarian propolis, curcumin and nigella (Yee & Koo, 2001; Stoicov & Houghton, 2013; Boyanova et al., 2003; Yanagawa et al., 2003; Kurauchi et al., 2019; Díaz-Gómez et al., 2013; Baltas et al., 2016; Vetvicka et al., 2016; Muniyappan et al., 2021; Khan et al., 2019b; Salem et al., 2010; Chahardoli et al., 2018). Plant extracts with biomedical potential, such as olive oil, licorice roots, and coconut oil, have piqued the interest of researchers, owing to their anti-inflammatory, anti-biotic, anti-oxidant, anti-microbial, anti-bacterial, antiplaque, and antiprotozoal activity, which can act as an antiulcer agent (Spósito et al., 2019; Karkanis et al., 2018; Pandey, 2017; Thakur & Raj, 2017; Ghani et al., 2018; Marina et al., 2009; Ngnameko et al., 2019; Romero et al., 2007; Foscolou et al., 2018; Wittschier et al, 2009; Wang et al., 2015; Hajiaghamohammadi et al., 2016; Meng et al., 2019; Dayrit, 2014).

Plant polyphenols and flavonoids such as Olive Oil in Fig. 2S-a-b-c inhibit VacA, a toxin secreted by the gastric pathogen *H. pylori*, therefore the polyphenols and flavonoids

displayed growth inhibitory effects on *H. pylori* (Gorzynik-Debicka et al., 2018; Tombola et al., 2003; El-Shouny et al., 2020; Modolo et al., 2015). Eradication of *H. pylori* remains a global issue due to the alarming increase of treatment resistance. Previous research has shown that *H. pylori* resistance to drugs rises. When reporting that there are several reasons for the failure of *H. pylori* eradication, the first (Major) is bacterial antibiotic resistance, and the second is that plant extracts were not able to completely kill and destroy *H. pylori*, but only hindered its growth. This is because plant extracts cannot reach the *H. pylori* that is located between the walls of the gastric mucosa, and it also does not rebuild the tissues of the stomach wall damaged by *H. pylori* (Fagoonee & Pellicano, 2019). Due to the incresing difficulties to eradicate *H. pylori* (Di Pierro et al., 2020; Haghighi et al., 2019), new and different approcahes have been proposed, Therefore Aim of the study:

Eco-friendly, Microwave Assisted Green Synthesis of Magnetic Fe@Au (Core-Shell) NPs to Enhance Olive oil Efficiency on Eradication of *H. pylori* because most of the nanoparticles that to be introduced to the human body acts as a therapeutic agent in (Fig. 1), if its size is less than 50 nm (Jeevanandam et al., 2018; Al-Radadi., 2022).

To evaluate the *in vivo* anti-*H. pylori* action of Fe@Au Core-Shell NPs with Olive oil, licorice roots and coconut oil (OLC) incorporated in a nanostructured drug delivery system. It is considered as a future treatment strategy with gastroprotective drug delivery systems.

2. Experimental details

2.1. Materials and method

Licorice root was bought from iHerb website, and washed thoroughly with distilled water. About 2 g sun-dried powder of root extract was boiled in 50 ml of sterilized water to get extract. Chloroauric chloride ($HAuCl_43H_2O$) was purchased from Sigma–Aldrich. A stock solution contains (1×10^{-3} M) auric salt and de-ionized water used for this process. Organic coconut oil was gotten from oil mill. Iron (III) chloride ($FeCl_3{\cdot}6H_2O$) was also purchased from Sigma–Aldrich. A stock solution contains (1×10^{-3} M) iron salt and de-ionized water and olive oil was gotten from farm in Aljouf.

2.2. Biosynthesis of gold coated iron nanoparticles (Fe@AuNPs)

To avoid any contamination in the results, before any reaction, all glassware was cleaned and sterilized. The synthesis consists of two main steps.

(1) Synthesis of Fe-NPs by adding 3 ml of (0.001 M) aqueous solution of $FeCl_3{\cdot}6H_2O$ to OLC extract (2 ml of olive oil stock, 2 ml of licorice extract, and 1 ml of stock solution of coconut oil), where is natural antioxidants acted as a reducing agent, the process was assisted by microwaves (CEM Discover Microwave™) for 60 min at 50 °C. The color transformation from light yellow to dark brown indicated the reduction of Fe^{3+} to Fe^0 nanoparticles.

(2) for synthesis of Au-NPs, 5 ml of (1×10^{-3} M) aqueous $HAuCl_4{\cdot}3H_2O$ solution was mixed with natural antioxidants, consist of 2 ml of licorice extract, 2 ml of olive oil and 1 ml of coconut oil. In addition, magnetic bar was put in the mixture and microwave radiations were provided for 60 min at 25 °C. The change in the color of solution from yellow to red, indicated the reduction process of Au^{3+} to Au^0 and formation of the gold nanoparticles. Subsequently, once the gold nanoparticles were formed, Fe-NPs were added to it for core shell nanoparticles and stabilized the mixture under microwave radiation for 10 min. Thus, the color transformation confirmed the synthesis of nanoparticles.

2.3. Characterization of Fe@Au nanoparticles

Due to combination of gold coated iron NPs (Fe@AuNPs), was morphologically characterized by a variety of spectroscopic techniques. The absorbance spectra were recorded using double beam scanning spectrophotometer and quartz cuvettes (Cary 100 UV–Vis Spectrometer from Agilent) at 350–700 nm. Fourier Transform Infrared Spectroscopy (FT-IR) (a Nicolet 6700) was performed in the spectral range of 200–4000 cm^{-1} and was utilized to determine the possible functional groups of the biomolecules that reside in the plant extract. The X-ray diffraction (XRD) (Shimadzu XRD-6000), were conducted to get data about the crystalline nature of nanoparticles. The internal structure of nanoparticles was examined by using Transmission electron microscope (TEM). Energy dispersive X-ray (EDX) (model-JSM-5610 LV) confirms the presence of gold and iron, demonstrating that the gold coated iron nanoparticles were formed. High Performance Liquid Chromatography (HPLC) analysis was performed to determine the percentage of natural antioxidants.

2.4. DPPH free radical scavenging assay

Protocol of (Choi et al., 2002) with minor modification was used to test the antioxidant potential of (OLC) extract and Fe@AuNPs. DPPH stock was prepared and 1 ml of (0.1 mM) DPPH methanolic solution was pipette out and gently mixed with 1 ml of (OLC) extract and Fe@AuNPs having varying Conc of (7, 31, 62, 125, 250 ,500 and 1000 μg/ml). The reaction mixture was incubated in the dark for half an hour and after incubation was exposed to absorbance at 517 nm against a blank solution. As a control 1 ml of methanol and 1 ml DPPH mixer was used. However, as a standard control butylated hydroxyl toluene (BHT) was used. The following formula was used to calculate the percent inhibition.

$$PI = \frac{AC - AT}{AC} \times 100$$

AC is the absorbance of control while AT is of sample and the values are calculated according to ascorbic acid reference.

2.5. Analysis of cytotoxicity of Fe@AuNPs with extract

A 20% of FBS (WELGEN Inc.), 20 μg/ml of bFGF, 100 units/ml of penicillin and 100 μg/ml of streptomycin supplemented with M199 medium was used to grow the human umbilical

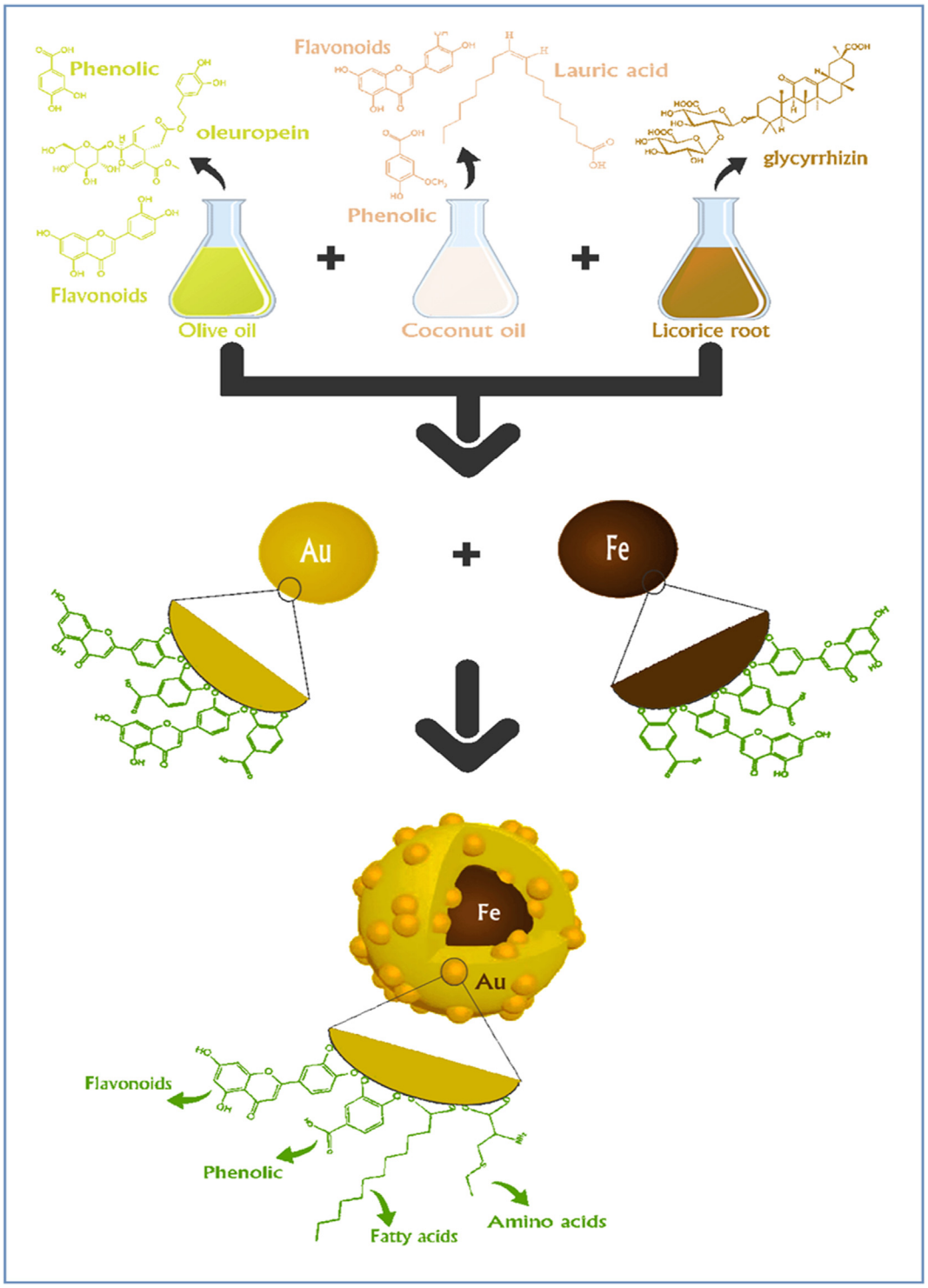

Fig. 1 A schematic of the OLC-Fe@AuNPs.

vein endothelial cells at 37°and 5% of CO_2. MTT assay was used to check the effect of (OLC) extract, and OLC-Fe@AuNPs on the viability of HUVECs. The basics of the MTT assay is the conversion of MTT (4,5-dimethylthiazol-2-yl) (2,5-diphenyl tetrazolium bromide) to insoluble MTT formazan. It happens by dehydrogenase which cleaved the tetrazolium ring in surviving cells. The process was performed in 24-well culture plates, after overnight incubation the M199 medium was supplemented with 1% of FBS and varying Conc of OLC extract and OLC-Fe@AuNPs solution followed by incubation for 24 h at 37° in humidified 5% carbon dioxide supplemented environment. Next, 5 mg/ml aqueous solution of MTT were added to each well and 0.3 ml additive DMSO was added to dissolve the MTT formazan quickly. The exper-

iment repeated three times and the treated samples were exposed to absorbance at 570 nm to measure the cell viability (Rodríguez-León et al., 2019).

$$\text{Cell viability Percentage } (\%) = \frac{\text{Sample Absorbance}}{\text{Control absorbance}} \times 100$$

2.6. Anti-ulcer (ulcer-preventive) activity study

To check the anti-ulcer activity of OLC-Fe@AuNPs, (OLC) extract, PBS, (Clarithromycin + Amoxicillin + Omeprazole) and ethanol, a total of 7 groups of Wister rats were enrolled in the study. PBS (10 ml·kg^{-1}) was administered orally to Group 1 for time period of 11 days and label it as control group. Group 2 were administered with PBS (10 ml·kg^{-1}) for 10 days and on the 11th day, absolute ethanol (5 ml·kg^{-1}) weas administered and labeled as ulcer control. Group 3 and 4 were respectively administered with 250 and 500 mg·kg^{-1} of OLC-Fe@AuNPs, while group 5 with triple regimen consisting of Clarithromycin 500 mg + Amoxicillin 1 g + 20 mg of Omeprazole for 10 days. Group 6 and 7 were respectively administered with 250 and 500 mg·kg^{-1} of (OLC) extract. After 1 complete day of fast, OLC-Fe@AuNPs or drug was administered at respective doses. After half an hour group 2–7 animals were administered with ethanol (5 ml·kg^{-1}) for induction of ulcer. All the animals were served with an aesthetic ether and scarified. Pylorus ligation method was used to measure gastric volumes. Under dissecting microscope each stomach was examined for gastric erosion. Gastric mucosal ulcer was measured by plane glass square length × width (10 × 10 mm) and the ulcerate area (UA) was calculated. The % of protection (P%) availed to the animals through various treatments was calculated using the formula:

$$\text{P\%} = \frac{(UA\ \ ulcer\ \ control - UA\ \ treatment)}{UA\ \ ulcer\ \ control} \times 100$$

Small piece of stomach was fixed in paraffin wax after measuring the ulcerate area. Using standard technique, 5 µm thick sections were cut in a microtome and kept on a glass slide and the tissues were stained with Hematoxylin-Eosin (H&E) stain and viewed under microscope. As previously mentioned in HPLC and Antioxidants, that the phytochemical studies of the extract of (OLC) proved the existence of flavonoids and phenolics, amino acids, fatty acids, peptides and vitamins.

3. Results and discussion

3.1. High performance liquid chromatography (HPLC)

Licorice root extract was used in combination with olive oil and coconut oil (OLC), the hydroxyl and alcoholic groups of OLC helped in reducing the Au^{3+} and Fe^{3+} ions, the OLC extract stabilizes the nanoparticles and helped in formation of bond between oxygen, iron and gold in biosynthesis of nanoparticles, in addition it has been used as an environmentally benign polymer. The three plant extracts (OLC) was considered a strong antibiotic for bacteria because they are rich in natural antioxidants such as amino acids, phenols, flavonoids, fatty acids and minerals such as (Fe, Ca, Na, K, Zn, S, Mg, P and Si) and vitamins such as (E, A, K and D), α-Tocopherol (E) and Retinol, these all acted as an anti-inflammatory agents, that restored damaged tissues to vitality and accelerates the healing of ulcers, and we found that one of the best plant extracts is the virgin olive oil: it is a powerful antibiotic for bacteria, it is considered to strengthen the immune system, protects the body from diseases and infections, prevents the oxidation of fats, prevents the formation of free radicals that cause cancerous tumors, increases gastric secretions and thus facilitates the process of absorption of natural antioxidants, and works to regulate the level of sugar in the blood, it slows the digestive process in the stomach, thereby helping to slow the increase in sugar level, it also contains natural antioxidants and a high amount of polyphenolic and flavonoids, it has more than forty compounds, as shown in Table 1 and Fig. 1S. Olive oil is also rich in saturated fatty acids, shown in Table 2, Figs. 2 and 3, such as palmitic acid, stearic acid and myristic acid, as well as unsaturated fatty acids. In addition, olive oil is very rich in phenols Fig. 2S (a-c) such as oleuropein, and also rich in three powerful natural antioxidants that are hydroxytyrosol, the vanillic acid, the verbascoside, and also contains a number of unsaturated fatty acids such as oleic acid, linoleic acid. The presence of green chlorophyll pigment (pheophytin) Fig. 3S, sterols and squalene Fig. 3S, it has also peptides. Olive oil is considered an antibiotic because it contains a high amount of triglycerides Fig. 3S, containing Retinol which restores damaged tissues. But olive oil lacks amino acids Table 3 and Fig. 4S that helps stabilize synthesized nanoparticles, and to improve the quality of olive oil and increase its efficiency as a plant extract, therefore we combined it with licorice root extract because it is rich in natural antioxidants such as carboxylic acids, and amino acids Table 3 and Fig. 4S, including glycerrhizin Fig. 5S, which has anti-ulcer activity, and its derivatives include carbenoxolone Fig. 5S, which has an effective affect in the treatment of ulcers of the stomach, duodenum and small intestine, anti-inflammatory, rich in phenols, flavonoids and steroids Fig. 6S, containing minerals, rich in aromatic compounds, and rich in proteins. Because of the damage and side effects already mentioned, due to high blood sugar level and fluid retention in the body Table.4, we added a small amount of it (2 ml) and combined it with coconut oil because it is rich in lauric acid and containing vitamin α-Tocopherol (E). It is a fatty acid Table.2 and is considered a strong antiparasitic, and strengthens the body's immunity by protecting it from many diseases, stimulator of beneficial bacteria, rich in vitamin E, which restores the vitality of damaged tissues and contains several vitamins including vitamin A as anti-inflammatory and stomach ulcer preventor and accelerates the healing of ulcers.

We carried out HPLC analysis of plant extracts to determine the percentage of natural antioxidants Table. 4 such as phenols, flavonoids, amino acids, fatty acids, vitamins and minerals. In Table. 5 proximate composition and energetic value of olive oil, coconut oil and licorice root has been mentioned. In Table.6 different sugars are listed. The studied amino acids are Glutamic acid, Valine, Alanine, Proline, Phenylalanine, Serine, Threonine, Glycine, Isoleucine, Methionine, Tyrosine, Leucine, Arginine, Lysine, Aspartic acid, Histidine and Cysteine. In OLC extract the oleic acids were found in between 35 and 67% and thus it is categorized the highest fatty acid present in the OLC extract, while Lauric, Linoleic, Myristic acid etc were found in trace amounts. Green synthesis of magnetic bimetallic nanoparticle (Core-Shell NPs) from iron ion solution and gold ion solution with plant

Table 1 OLC Compounds Concentration (mg/g).

Phenolic					
Concentration in Olive oil	Tyrosol	Caffeic acid	Oleuropein	Protocatechulic	
	11.04	12.1	39.56	9.55	
Retention time	10.5	8.0	14.02	13.5	
Flavonoids					
Concentration in Olive oil	Luteolin	Rutin	Kampherol	Querestein	
	15.7	30.12	19.27	9.77	
Retention time	13.2	5.4	10.3	15.02	
Phenolic					
Concentration in Coconut oil	Coumaric	Caffeic acid	Syringic	Vanillic acid	Gallic
	8.14	4.01	9.16	29.56	18.12
Retention time	5.0	8.2	9.3	11.6	12.5
Flavonoids					
Concentration in Coconut oil	Luteolin	Rutin	Isoquerestin		
	25.14	15.02	7.44		
Retention time	13.2	5.39	8.01		
Phenolic					
Concentration in licorice root	Sinapic	Ellagic	Protocatechulic	Ferulic	
	25.14	18.09	9.12	7.04	
Retention time	11.02	6.2	13.5	7.5	
Flavonoids					
Concentration in licorice root	Luteolin	Rutin	Kampherol		
	50.15	27.1	12.5		
Retention time	13.1	5.4	10.3		
Glycosides					
Concentration in licorice root	linamarin	pinoresinol	laricinesol		
	50.12	18.30	4.22		
Retention time	6.8	9.5	6.8		
Organic acids					
Concentration in licorice root	Succinic acid	Ascorbic acid	Fumaric acid	Gallic acid	
	13.41	10.87	2.17	4.56	
Retention time	9.1	11.0	10.7	4.21	
Triterpenes					
Concentration in licorice root	Glycyrrhizin				
	81.737				
Retention time	8.112				

extracts olive oil, licorice root and coconut oil, with the help of microwave oven without polymer or organic solvent in the medium interaction. Microwave-assisted synthesis of NPs is electromagnetic and showing spectrum with frequency of (300) MHz to (300) GHz (TEM Discover Microwave™), it depends on electromagnetic radiation that relies on heating the solution directly with high efficiency and proves the dissolution of the reactants and the formation and growth of a rapid and homogeneous nucleus in Fe@AuNPs, which improves reaction conditions, green synthesis of NPs occur in one step, fast and short time to reduce the chance of side reactions, giving pure NPs, and producing high degree of dispersion of surface morphology, and stabilizing nanoparticles by prevent the aggregation as shown in Fig. 7. The surface area was large and produced small sized nanoparticles, finally, in an environmental friendly and safe manner that does not result in the generation of toxic or harmful waste. In medical sector gold nanoparticles drawn a significant consideration due to its potential biomedical applications. Fe@AuNPs were biosynthesized in the current study using OLC as a capping and reducing agent assisted by microwave radiation. Furthermore, factors such as metallic salt concentration and microwave radiation that affecting the synthesis of NPs were also studied. Synthesis of nanoparticles were confirmed by the color transformation to dark reddish brown and it was monitored by UV Spectroscopy (El-Naggar et al., 2016; Al-Radadi, 2021b).

3.2. Factors affecting the synthesis of AuNPs

3.2.1. Volume of extract and volume of Au metal

The biosynthesis of gold nanoparticles was confirmed by UV–Vis absorption spectroscopy. Fig. 4A, is the UV spectra of microwave assisted and OLC mediated gold nanoparticles. Olive oil was taken in quantities of 0.5, 1, 1.5 and 2 ml. whereas, licorice root extract and coconut oil was taken in quantities of 2 ml and 1 ml. A gradual increase in the absorbance intensity was observed by increasing the OLC Conc. from 0.5 ml to 2 ml, maximum peaks were observed at 2 ml, some minor peaks were also observed that corresponds to the presence of trace biomolecules in the extract. In the case

Table 2 Composition in fatty acids (saturated and unsaturated) for olive oil, coconut oil and licorice root.

Fatty acid	Caprylic (C8)	Capric (C10)	Lauric (C12)	Myristic (C14)
Olive oil content (%)	0.0	0.0	0.13	0.0
Coconut oil content (%)	6.54	9.21	46.75	16.96
Licorice root content (%)	0.0	0.0	0.21	4.08
Retention time(min)	22.3	24.9	26.1	26.8
Fatty acid	Pentadecanoic (C15)	Palmitic (C16)	Palmitoleic (C16:1)	Heptadecanoic (C17)
Olive oil content (%)	0.0	14.25	0.0	2.26
Coconut oil content (%)	0.47	9.61	0.0	0.34
Licorice root content (%)	1.89	25.36	0.27	2.26
Retention time(min)	27.9	30.2	30.9	31.7
Fatty acid	Stearic (C18)	Oleic (C18:1)	Linoleic (C18:2)	Linolenic (C18:3)
Olive oil content (%)	1.61	66.69	16.34	0.56
Coconut oil content (%)	1.29	7.62	0.0	0.0
Licorice root content (%)	7.63	35.72	10.83	3.24
Retention time(min)	33.8	35.7	37.2	40.04
Fatty acid	Arachidic (C20)	Arachidonic (C20:1)	Behenic (C22)	Lignoceric (C24)
Olive oil content (%)	0.0	0.0	0.05	0.04
Coconut oil content (%)	0.23	0.0	0.0	0.0
Licorice root content (%)	8.16	0.35	0.0	0.0
Retention time(min)	39.4	39.8	42.3	43.1

0 : undetected.

of $HAuCl_4$ concentration, in Fig. 4B it was taken in different quantities of 1, 2, 3, 4 and 5 ml, where the results showed increasing in the intensity of absorbance with increasing in volume, the highest absorption was observed at maximum wavelength of 540 nm at 5 ml of extract. The color change from yellow to red was the primary indication of the biosynthesis of Au-NPs with ideal SPR peaks, at low volumes the broadened peak was observed which confirm the presence of large sized Au-NPs (Al-Radadi, 2022).

3.2.2. The effect of time on AuNPs

In Fig. 4C, the gold nanoparticles gave a characteristic peak at 540 nm which confirmed its synthesis again and proved the OLC extracts are good capping and reducing agents. However when the time exposure of microwave radiation increased from 60 to 70 min, sharpness of peak was observed which indicated the stability and maximum size of the nanoparticles.

3.2.3. The effect of pH on AuNPs stability

The UV–visible spectra of gold nanoparticles displayed in Fig. 4D with different pH factors investigated, it was found that the most preferable pH for extract (OLC) was pH = 6 at λ_{max} = 540 nm, which gave sharper and higher absorbance peak and confirmed by TEM images indicating that at this pH value the gold nanoparticles were more homogeneous shape with smaller size (Al-Radadi & Al-Youbi, 2018a), In contrast to pH values below 6, the particles size was found large due to agglomeration.

3.2.4. The effect of temperature on AuNPs

Temperature is one of the important parameters in the synthesis of nanoparticles. Different peaks were observed at (15, 20, 25 and 30 °C). A narrow UV band at 540 nm was observed at temperature of 25°, while the absorbance intensity became weaken at 30 °C as shown in Fig. 4E. The increase in temperature above than 25°resulted in aggregation of nanoparticles and thus the peaks became weaken. The best synthesis of nanoparticles was observed at 25°.

3.3. Factors affecting on the synthesis of FeNPs

3.3.1. Volume of extract and volume of Fe metal

Fig. 5A shows the UV–visible absorption spectrum of iron nanoparticles at a spectral range of 150–650 nm (Pattanayak & Nayak, 2013). In addition, the absorption spectra of the synthesized Fe^0 nanoparticles it varies with the amount of iron from 1 to 5 ml. Where several absorption peaks were observed at 220 nm at 1 ml, 225 nm at 2 ml, 250 nm at 3,4 and 5 ml due to the excitation of surface plasmon vibrations in the FeNPs solution. The highest absorption was observed at 3 ml and is the indication of the small Fe nanoparticles (Carroll et al., 2010; Hosseynizadeh Khezri et al., 2012).

The extract was prepared as previously presented with gold in terms of quantities taken from licorice root extract, olive oil and coconut oil. The UV–visible absorption spectrum of (OLC) extract in Fig. 5B showed suitable (SPR) to synthesize the iron nanoparticles via high UV spectra at 5 ml..

3.3.2. The effect of time on FeNPs

The time factor was studied during preparing iron nanoparticles, where the results in Fig. 5C showed that the best time it took to prepare iron nanoparticles in the microwave was 60 min, where a change in color was observed from yellow to brown, indicated the formation of small Fe nanoparticles. It was also observed that the reactivity of FeNPs was high, which confirms the small size of the Fe^0 nanoparticles, because

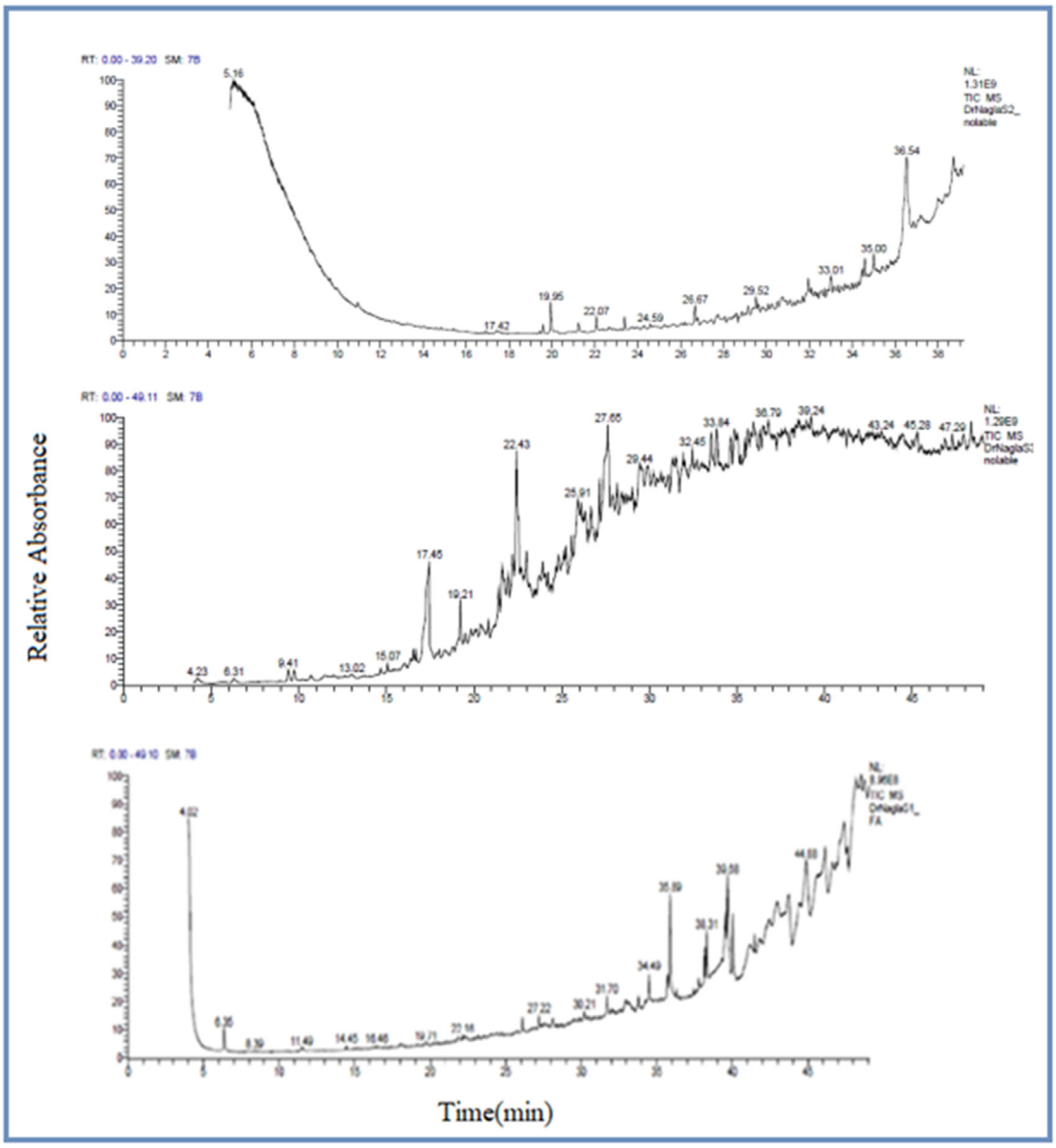

Fig. 2 Mass spectrum of the main fatty acid compounds in the Olive oil, Coconut oil and Licorice root.

it is linked to their particle size: smaller sizes lead to higher reactivities (Machado et al., 2014). Hence, the nanoparticles was prevented from agglomerating.

3.3.3. The effect of pH on FeNPs stability

The pH was determined by using digital pH meter. The pH of the reduced Fe nanoparticle solution found to be 6. The pH factor of the Fe nanoparticles was studied as shown in Fig. 5D, by adding hydrochloric acid or sodium hydroxide to obtain the best results. It was observed that the natural pH = 6 is the preferable and standard pH for synthesis of FeNPs.

3.3.4. The effect of temperature on FeNPs

A narrow UV band at 250 nm was observed at temperature of 50°, while the absorbance intensity became weaken at 70 °C as shown in Fig. 5E. The increase in temperature above than 50° resulted in the aggregation of nanoparticles, and thus the peaks became weaken. The best synthesis of nanoparticles was observed at 50°. At 70 °C the SPR peak decreased.

3.4. The UV–Vis spectrum of Fe@AuNPs synthesized using microwave radiation

The Fe@AuNPs was first characterized by UV–Vis Spectroscopy as shown in Fig. 6 It is observed that FeNPs showed a prominent absorption peak at λ_{max} = 279 nm, whereas AuNPs displayed an characteristic peak at λ_{max} = 565 nm A red shift was also observed in the peak for Fe@AuNPs as shown in Fig. 6. The bathochromic shift indicated the large sized OLC mediated nanoparticles (Bandyopadhyay et al., 2014)

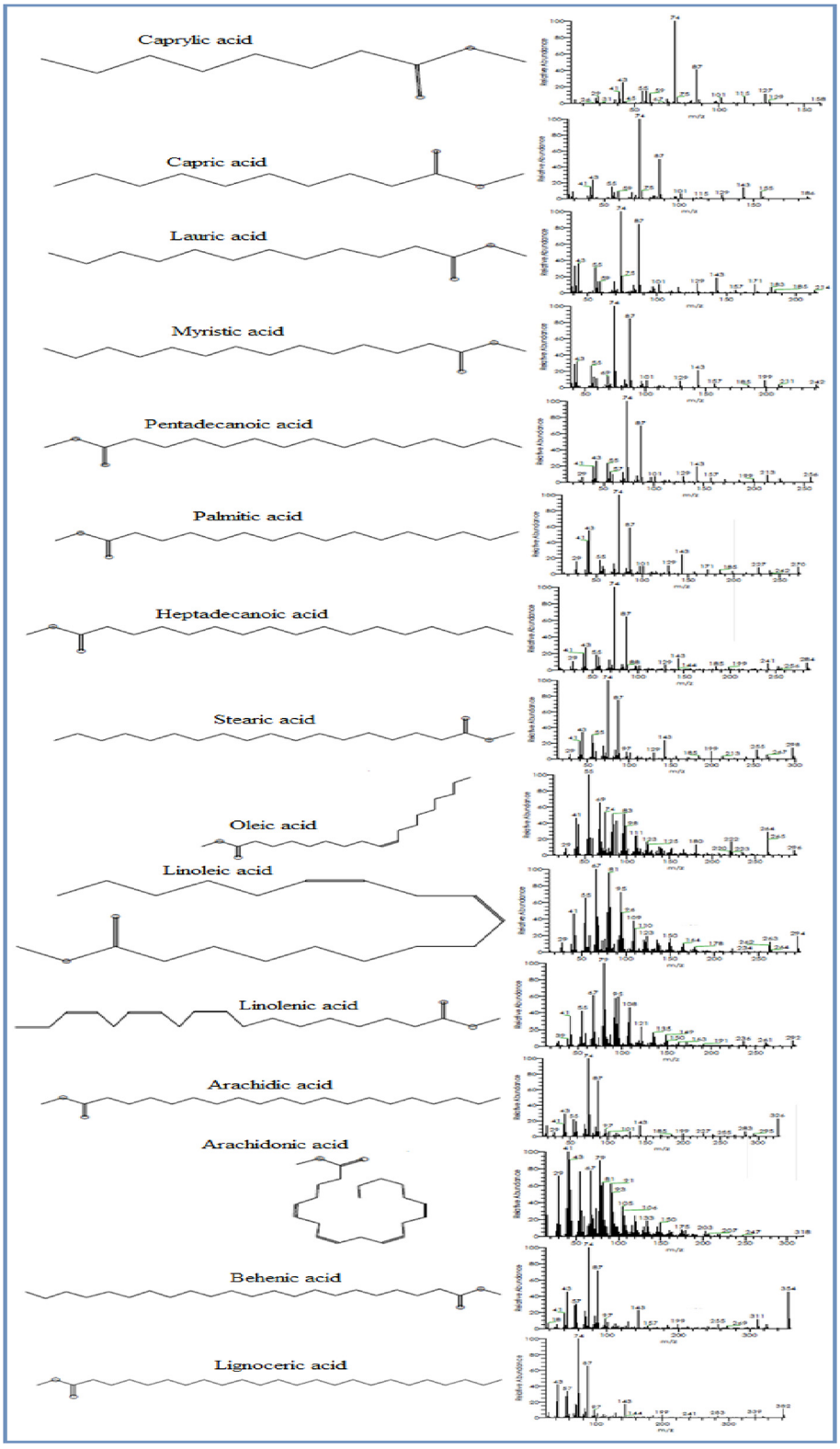

Fig. 3 Mass Fragmentation and Chemical structure of the main fatty acid compounds in the Olive oil, Coconut oil and Licorice root.

3.5. Transmission electron microscopic analysis (TEM) and HR-TEM of Fe@AuNPs

This special type of microscopy was used to determine the shape and size of core–shell iron and gold nanoparticles. The TEM image illustrated and confirmed that the core–shell iron and gold nanoparticles were spherical in shape, homogeneous, not aggregated and small in size (Al-Radadi, 2021b). The size of the nanoparticles was 2.9, 3.4, 5.7 and 10 nm as shown in Fig. 7, and the HR-TEM micrograph of spherical Fe@AuNPs

Table 3 Concentration of amino acids (mg/100 g) essential and non-essential present with in Olive oil, coconut oil and Licorice root extract.

Coconut oil	Olive oil	Licorice root	RT (min.)	Amino acids
Essential Amino Acids (EAA) (mg/100 g)				
0	0	9.66	19.2	L-Threonine
0	0	10.25	24.8	L-Valine
0	0	5.69	27.7	L-IsoLeucine
0	0	12.78	31.9	L-Methionine
0	0	5.26	42.3	L-Phenyl alanine
0	0	2.8	51.3	L-Leucine
0	0	7.23	58.7	L-Lysine
Non-Essential Amino Acids (NAA) (mg/100 g)				
0	0	9.24	12.8	Aspartic acid
0	0	4.98	20.6	Arginine
0	0	10.45	28.9	Glutamic acid
0	0	8.82	40.1	Glycine
0	0	5.24	42.2	Alanine
0	0	6.21	47.6	Proline
0	0	–	58.5	Tyrosine
0	0	7.19	52.4	Serine
0	0	3.76	50.2	Histidine
0	0	8.07	59.7	Cysteine

Table 4 Antioxidant activity, total phenolic content and total flavonoids content of olive oil, coconut oil and licorice root.

Antioxidant	total phenolic	total flavonoids	DPPH	ABTS
	(mg/g)	(mg/g)	(μg/ml)	(μg/ml)
Olive oil	**27.4 ± 1.92**	9.2 ± 1.48	301.2 ± 34.8	458.4 ± 38.2
Coconut oil	3.25 ± 0.31	5.42 ± 0.64	405.0 ± 30.1	549.3 ± 40.5
Licorice root	15.26 ± 0.72	**25.14 ± 1.98**	**86.9 ± 23.7**	**63.4 ± 9.3**

Table 5 Proximate composition and Energetic value of coconut oil and olive oil.

Proximate composition	Ash	Moisture	Total Proteins	Total Lipids	Total Carbohydrates	Total Cholesterol	Triglycerides
	(g/100 mg dry weight)	(g/100 mg dry weight)	(g/mg dry weight)	(mg/g)	(g/mg dry weight)	(mg/gm)	(mg/gm)
Olive oil content	0.35	4.51	0.19 ± 0.05	989.4 ± 5.7	0.0	0.19 ± 0.05	2.41 ± 0.23
Coconut oil content	0.14	7.2	1.04 ± 0.42	958.2 ± 7.4	0.0	0.52 ± 0.14	0.91 ± 0.15
Licorice root content	17.22	16.4	21.42 ± 0.94	87.1 ± 9.5	24.51 ± 31.3	–	–

is shown in Fig. 8A. The HAADF-STEM images of the Fe@Au nanoparticles and the elemental mapping images is shown in the Fig. 8B that clearly demonstrates the Fe core and Au shell in a bright and dark contrast, which can be further verified by corresponding energy dispersive x-ray spectroscopy (EDX) in Fig. 11B (Wu et al., 2009). By the analysis of size distribution histogram the size of the nanoparticles was determined and shown in Fig. 8C (Chung & Shih, 2014).

3.6. X-ray diffraction (XRD) of Fe@AuNPs

The X-ray diffraction (XRD) pattern in Fig. 9 illustrated the OLC mediated nanoparticles are crystalline in nature (Al-Radadi & Al-Youbi, 2018b) and showed characteristic peaks at scattering angles of (2θ) values of 38.13°, 44.23°, 64.71°, and 77.49°, which was indexed to (111), (200), (220), (311) (Singh et al., 2013). In addition, the (XRD) of iron nanoparti-

Table 6 Sugars composition for olive oil, coconut oil and licorice root (mg/100 g).

Sugars	Sucrose	glucose	Xylose	Arabinose	mannose
Olive oil	0.0	0.0	0.0	0.0	0.0
Coconut oil	0.0	0.0	0.0	0.0	0.0
Licorice root	149.6	57.2	0.0	0.0	0.0
Retention time(min)	8.8	7.9	3.5	5.3	6.2

Sugars	galactose	Lactose	Rhamnose	fructose
Olive oil	0.0	0.0	0.0	0.0
Coconut oil	0.0	0.0	0.0	0.0
Licorice root content	1.3	0.0	0.0	4.1
Retention time (min)	7	9.5	10.5	4.7

cle showed characteristic peaks at scattering angles (2θ) values of 43.7°, 62.5°, which was indexed to (1 1 0), (2 0 0). Also, the (XRD) of Fe@AuNPs, due to overlap of diffraction peaks the iron peaks are under the gold at 2θ = 54.37°, 58.12°, 70.31, and 78.13° as shown above (Zhang et al., 2006; Kvitek et al., 2019). The average crystallite size according to Debye–Scherrer equation $D = \frac{k\lambda}{\beta cos\theta}$ was calculated and found to be 5.5 nm.

3.7. Fourier transform infrared spectroscopy (FTIR) of Fe@AuNPs

FT-IR analysis were conducted to know about the possible involvement of OLC extract functional groups in the synthesis and reduction of iron and gold nanoparticles, the FT-IR spectra of NPs were compared against spectra of extract. Multiple characteristic peaks were observed for extract between 400 and cm^{-1}4000 cm^{-1} as in shown in Fig. 10. The bands shown at 3712.5 cm^{-1} was due to the stretching and vibrations of alcohol (O—H) bonds, the peaks at 3472 cm^{-1} indicates the existence of primary amino bond, 3267 cm^{-1} indicates to aromatic carbon ring, and the (C—H) aliphatic group at 2921.8 cm^{-1} supports that fatty acids in olive oil and coconut oil are long-chain carboxylic acids. The strong peak at 1733 cm^{-1} corresponds to carbonyl group (C═O) bond stretching, disappearance and vibration of flavonoids and polyphenols present in the OLC extract. Due to the coordination and reduction of bio-molecules with Au, a small shift was observed towards lesser wave numbers for the above described peaks (Kumaret al., 2021; Ahmad et al., 2015). The peak at 1025 cm^{-1} indicates the existence of (C—N), similar characteristic peaks of FeNPs with extract were also observed. Also, similar peaks at 3587, 3148, and 1337 cm^{-1} appeared in the FT-IR spectra of Fe@AuNPs with extract and thus indicating the presence of similar functional groups in the capping of iron nanoparticles.

3.8. Energy dispersive X-ray spectroscopy (EDX) of Fe@AuNPs

Elemental composition of the nanoparticles was estimated by EDX, confirms the presence of gold nanoparticles were produced by reduction of the Au^{3+} ions, in addition, presence of iron nanoparticles by reduction of the Fe^{3+} ions. The EDX image showed the core–shell structure, the Au is distributed around the whole Fe core, as manifested by the line scanning image in which only Au appears in the external edges, while Fe show up in the middle, as shown in Fig. 11B, Au ligands are stronger than those of Fe, indicating the higher content of Au in the nanoparticles, where the atomic ratio of Au against Fe is roughly 70:30. EDX spectrum Fig. 11A shows the presence of additional carbon, oxygen, calcium and potassium (Ban et al., 2005).

3.9. Magnetic hysteresis loops of Fe@AuNPs

Fig. 12 Illustrated the prepared Fe@AuNPs has magnetic characteristic due to the presence of iron nanoparticles. The magnetic nanoparticles were designed to target affected tissue by applying an magnetic field (Liu et al., 2020), the magnetic properties were confirmed and studied by measuring hysteresis loops at 25 °C. As in Fig. 12A the magnetization vs the applied magnetic field curve, the Fe@AuNPs showed characteristic superparamagnetic behavior and high saturation fields around 36.25 amu/g (Pana et al., 2007). At room and ordinary temperatures, the Fe@Au core–shell nanoparticles are ferromagnetic in nature (Ban et al., 2005). Taking into consideration that ferromagnetic minerals tend to produce narrow loops (Mooney, 2002), and the results showed that Fe@AuNPs are the narrower loop compared to other minerals (Ovejero et al., 2015). The image of the magnetic nanoparticles is shown in Fig. 12B.

3.10. Biological activity

3.10.1. Antioxidant activity of Fe@AuNPs with extract

It is revealed from different studies that phenolic compounds in the (OLC) extract acts as an antioxidant and reducer of $FeCl_3{\cdot}6H_2O$ and $HAuCl_4$ to Fe@AuNPs. Free radicals usually damage the cells and tissues therefore the role of antioxidant is very important. Recently natural plant as a source of antioxidants was widely used to determine the antioxidant potential of nanoparticles usually DPPH was used (Vijaya Kumar et al., 2018). Upon reduction of DPPH the color of iron transform into brown, and the color of gold changes to red. The color transformation is due to production of H^+ ions (Adawiyah et al., 2019). In Fig. 13A, it was found that the DPPH scavenging activity increases with the increase of the concentration of (OLC) and Fe@AuNPs, due to inhibition

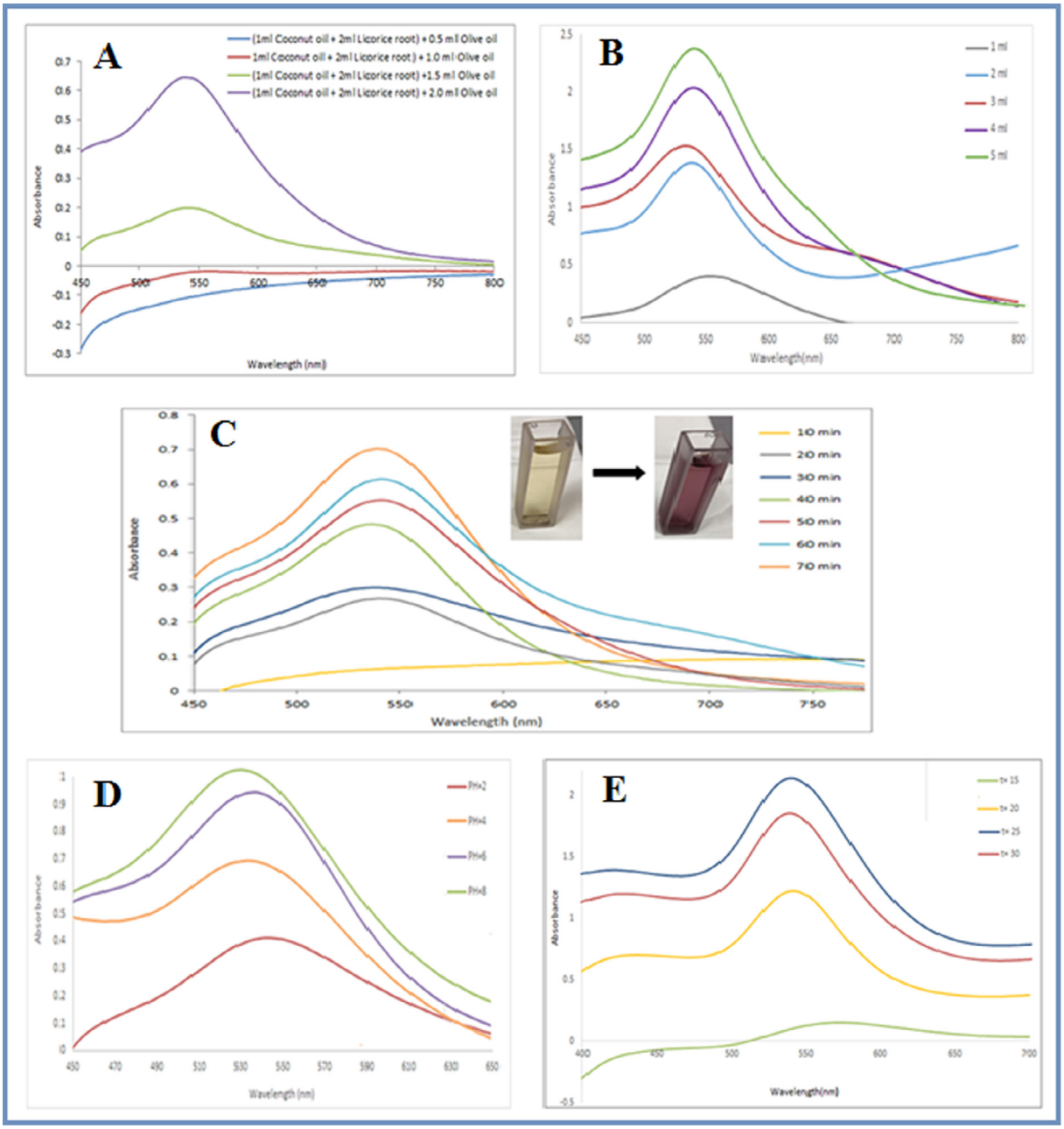

Fig. 4 (A) UV–visible spectrum of AuNPs synthesized using various volumes [(1 ml Coconut oil + 2 ml Licorice root) + (0.5–2.0 ml Olive oil)] with 5 ml 1×10^{-3} M $HAuCl_4$ solution after 60 min. (B) UV–visible spectrum of AuNPs produced via various volumes (1–5) ml 1×10^{-3} M $HAuCl_4$ solution with 5 ml extract after 60 min. (C) UV–visible spectrum of AuNPs as a task of 5 ml 1×10^{-3} M $HAuCl_4$ solution and 5 ml of extract after 60 min of addition. (D) UV–Vis spectra as a purpose of effect of different (2–8) pH of 5 ml 1×10^{-3} M $HAuCl_4$ solution and 5 ml of extract after 60 min. (E)UV–visible spectrum of AuNPs as a task of 5 ml 1×10^{-3} M $HAuCl_4$ solution and 5 ml of extract after 60 min. as a function of temperature (15–30 °C).

of the interaction with free radicals. Antioxidant activities of the compounds, present in the extract may depend on structural features, such as the number of phenolic or methoxy groups and flavones hydroxyl. The synthesized Fe@AuNPs showed scavenging of DPPH free radicals (Francis et al., 2018; Vijayan et al., 2018; Abdoli et al., 2021).

Owing its capability to cape free radicals, DPPH antioxidant assay is widely used technique DPPH when encounters antioxidants, it retrieved the hydrogen ions A purple color is produce as a result and can be detected at 517 nm (Shunmugam, et al., 2021). DPPH is more stabilized when it gets more hydrogen ions and upon proper reduction its initial purple color changes from purple to yellow and thus DPPH gets stabilized DPPH free radical scavenging effect of (OLC) and Fe@AuNPs with extract in varying Cons of (0, 1, 3, 7, 15, 31, 62, 125, 250, 500, and 1000 μg/ml) indicated impressive prevention similar to BHT. The IC_{50} of (OLC), BHT, and Fe@AuNPs with extract was found 404, 370, and 248 μg/ml,

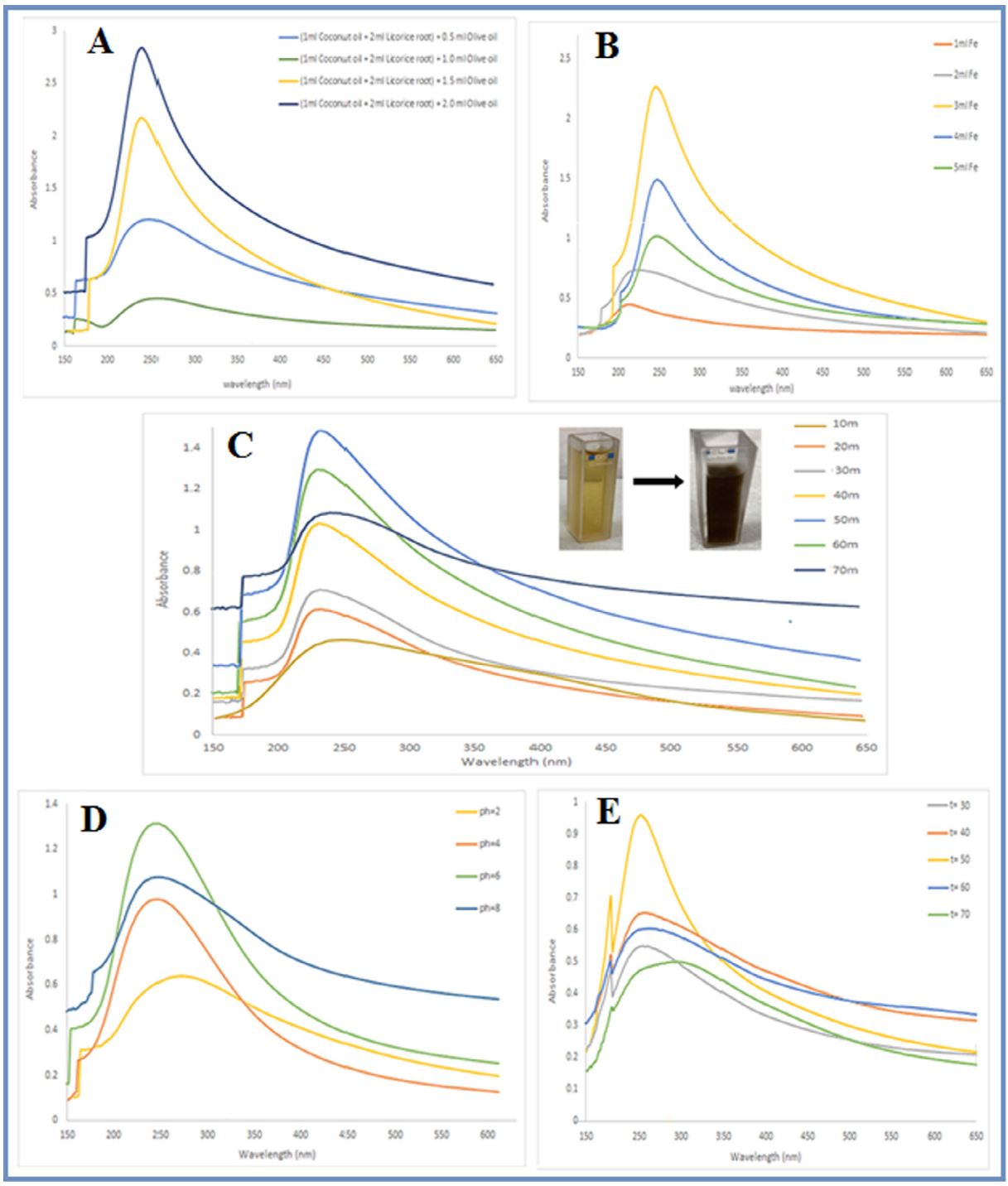

Fig. 5 (A) UV–visible spectrum of FeNPs produced via various volumes (1 ml Coconut oil + 2 ml Licorice root) + (0.5–2.0 ml Olive oil) with 3 ml 1×10^{-3} $FeCl_3{\cdot}6H_2O$ solution after 60 min. (B)UV–visible spectrum of FeNPs produced via various volumes (1–5) ml 1×10^{-3} M $FeCl_3{\cdot}6H_2O$ solution with 5 ml extract after 60 min. (C) UV–visible spectrum of FeNPs as a task of 3 ml 1×10^{-3} M $FeCl_3{\cdot}6H_2O$ solution and 5 ml of extract after 60 min. (D) FeNPs UV–Vis spectra as a purpose of effect of different (2,4,6 and 8) pH of 3 ml 1×10^{-3} $FeCl_3{\cdot}6H_2O$ solution and 5 ml of extract after 60 min. (E) UV–visible spectrum of FeNPs as a task of 3 ml 1×10^{-3} $FeCl_3{\cdot}6H_2O$ solution and 5 ml of extract. as a function of temperature (30–70 °C).

respectively (kumar et al., 2021; Al-Radadi, 2021a) as shown in Fig. 13A. In correspondence to our studies, previous studies have reported potential antioxidant activities by using metallic nanoparticles.

3.10.2. Cytotoxicity survey of Fe@AuNPs with extract

Test cells (HUVEC) were treated with varying Cons of (OLC) and OLC-Fe@AuNPs extract and cytotoxicity were determined by MTT assay. After incubation of 48 h the activity

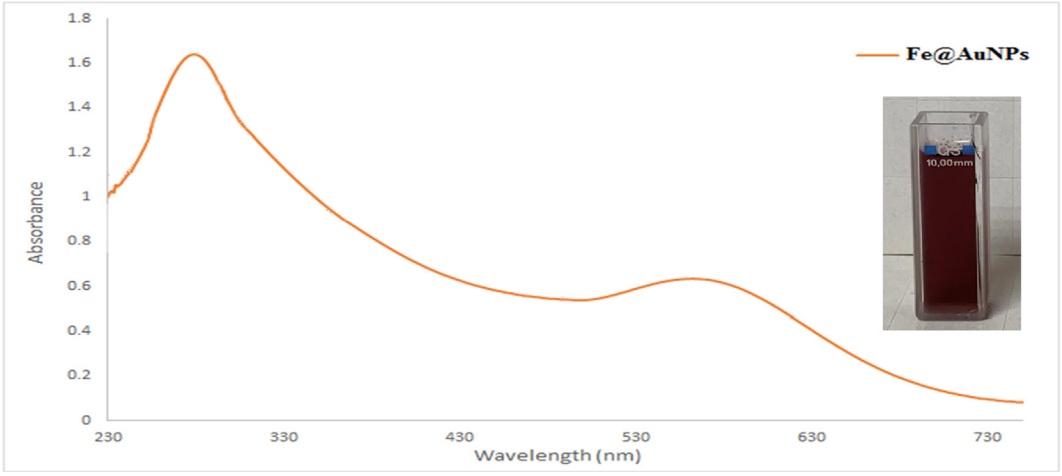

Fig. 6 UV–visible spectrum of Fe@AuNPs with (OLC) extract after 10 min.

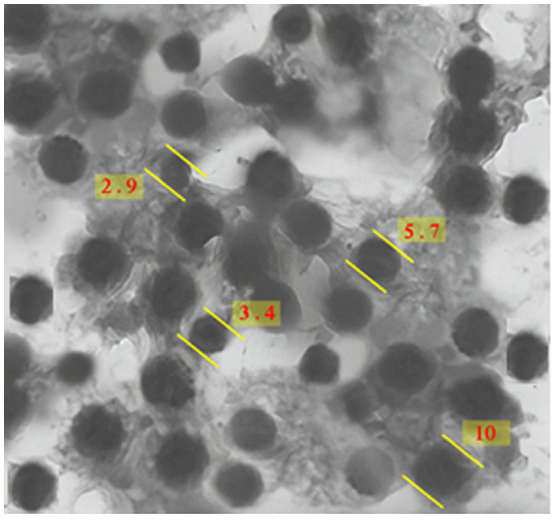

Fig. 7 Transmission electron microscopy (TEM) micrograph of iron coated with gold nanoparticle.

were detected at absorbance rate of 570 nm, which showed extra ordinary compatibility even at highest concentration of 1000 µg/ml of (OLC) and Fe@AuNPs as shown in Fig. 13B. previously studies has reported that combination of biological compounds with metals in nanoparticles reduce its cytotoxicity (Kandasamy et al., 2021, Mohammadi et al., 2021).

3.10.3. Antimicrobial activity

Antimicrobial activities of the (OLC) extract and Fe@AuNPs and control was evaluated against bacteria and fungi. Conventional paper disk diffusion method was used to determine the inhibition zones and MIC values. As a positive controls Norfloxacin, and Nystatin were used. The results were represented in Tables 7 and 8. The OLC extract showed IZ near to Norfloxacin, and Nystatin, while, Fe@AuNPs showed potential zones of inhibition against test organisms as compared to drug of reference. OLC extract exhibited moderate to potent antibacterial activities with inhibition zone (IZ) ranged between 22 and 30 mm for *Bacillus subtilis* and *Escherichia coli* compared with that of norfloxacin that have IZ ranged between 24 and 27 mm. Moreover, Fe@AuNPs showed potent IZ between 28 and 29 mm for *Bacillus subtilis* and *Salmonella typhi*. For fungi the (OLC) extract was presented antifungal activity with inhibition zone (IZ) ranging between 18 and 19 mm for *Fusarium oxysporum, Aspergillus flavus* and *Penicillium citrinum*. In comparison to nystatin as a therapeutic antifungal agent (17–20 mm). Moreover, Fe@AuNPs showed IZ great results more than the standard drug between 21 and 22 mm for *Aspergillus niger* and *Fusarium oxysporum*. The minimal inhibition concentration (MIC) for (OLC) extract with antibacterial potential was ranged between 3.9 µg/mL and 15.62 µg/mL against *Salmonella typhi* and *Bacillus subtilis* respectively. From the other hand Fe@AuNPs showed promising MIC which ranged between 0.03 µg/mL and 6.56 µg/mL against *Salmonella typhi* and *Bacillus subtilis*, respectively. In case of antifungal activity MIC for (OLC) extract the results were ranged between 15.62 µg/mL and 62.5 µg/mL toward *Aspergillus niger* and *Fusarium oxysporum*, respectively. At the same time Fe@AuNPs showing 6.56 µg/mL and 13.5 µg/mL against *Candida albicans* and *Aspergillus niger*, respectively. This result was the highest than the nystatin (standard drug) which recorded MIC against *Candida albicans* and *Aspergillus niger* as 7.81 µg/mL and 20.5 µg/mL, respectively. As previously mentioned in HPLC and antioxidants that the (OLC) extract contained large amounts of natural, phenolic, flavonoids, vitamins, fatty acids, amino acids, peptides and minerals. The presence of multiple phenolic and flavonoids have shown many health-promoting benefits such as anticancer, anti-inflammatory, anti-ulcer, antibacterial and antifungal (Al-Radadi, 2021a; Wang et al., 2015) and that is consider the main reason and interpretation for the antimicrobial activity for (OLC) extract. Against multiple microorganisms the antibacterial potential of OLC were evaluated (Sarwar et al., 2020). *Burkholderia cepacia* and *Klebsiella pneumonia* is inhibited by Myricetin, while flavonoids kaempferol and myricetin are also have the potential to cure gastric ulcers. anti-*Helicobacter pylori* activity is also possessed by these compounds and thus used as a potent agent in therapeutics (Sharifi et al., 2019). Echinacin-permethyl ether and apigenin-5,4-dimethyl ether are the derivatives of echinacin and apigenin-7-O-glucoside per methylate which is formed by their methyla-

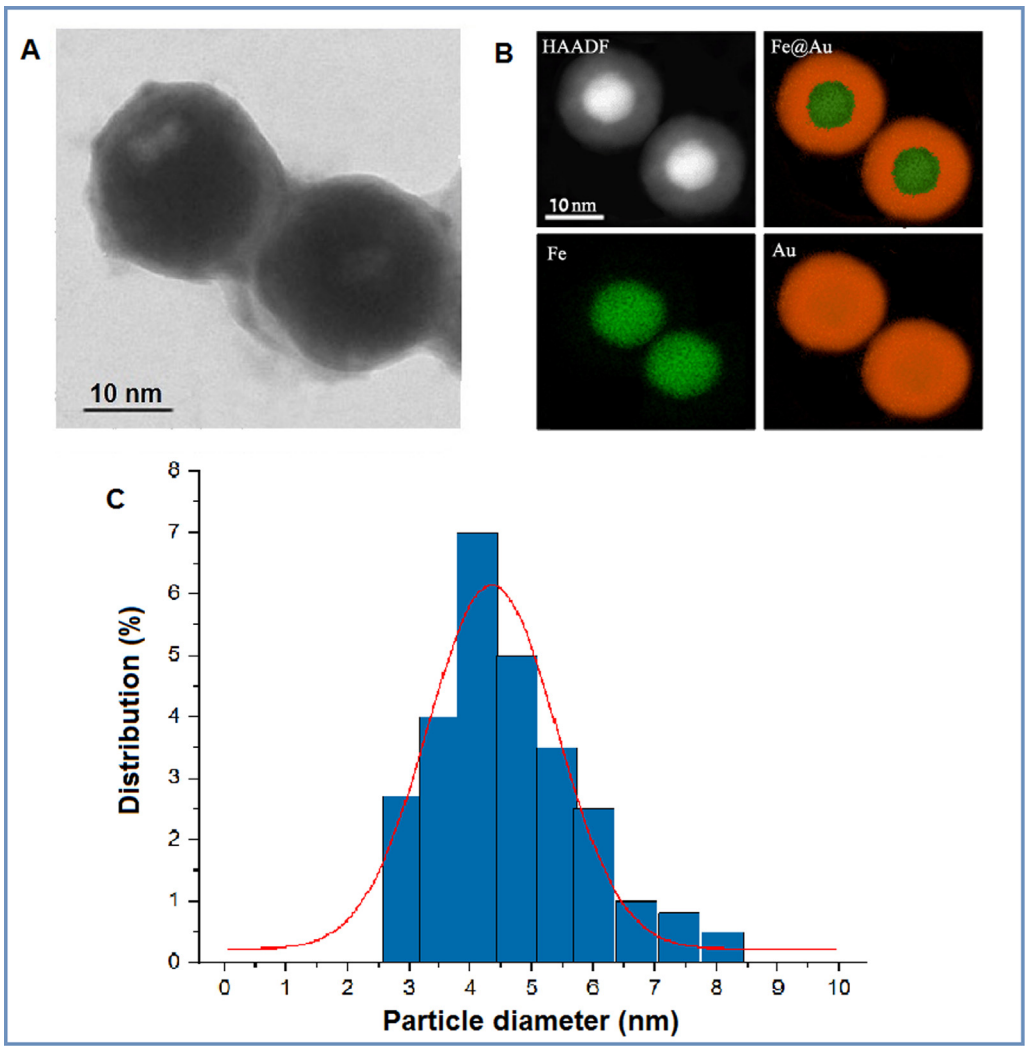

Fig. 8 (A) HR-TEM image of spherical Fe@AuNPs, (B) HAADF-STEM images of the Fe@AuNPs and the elemental mapping images and (C) Size distributions of Fe@AuNPs.

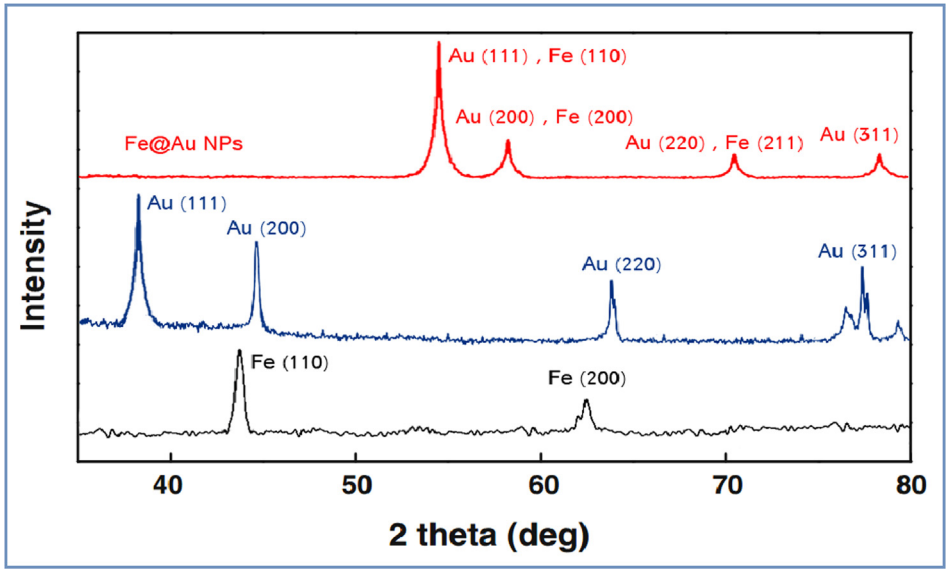

Fig. 9 X-ray diffraction (XRD) patterns of green synthesized iron, gold, and Core-Shell Iron@Gold Nanoparticles.

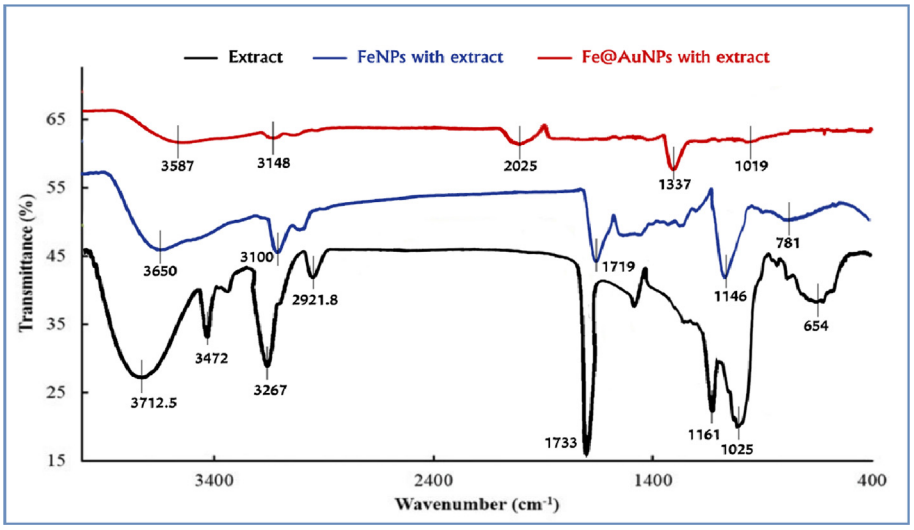

Fig. 10 FT-IR spectra of olive oil and coconut oil and Glycyrrhiza root extract, FeNPs with aqueous extract and Fe@AuNPs with aqueous extract.

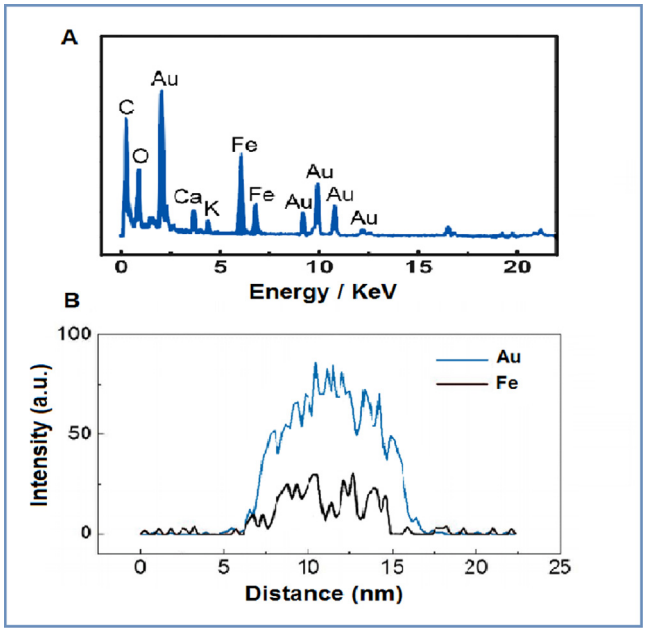

Fig. 11 (A) Energy-dispersive X-ray spectroscopy (EDX) spectrum of Fe@AuNPs with aqueous extract and (B) Line scanning profiles of Fe@AuNPs.

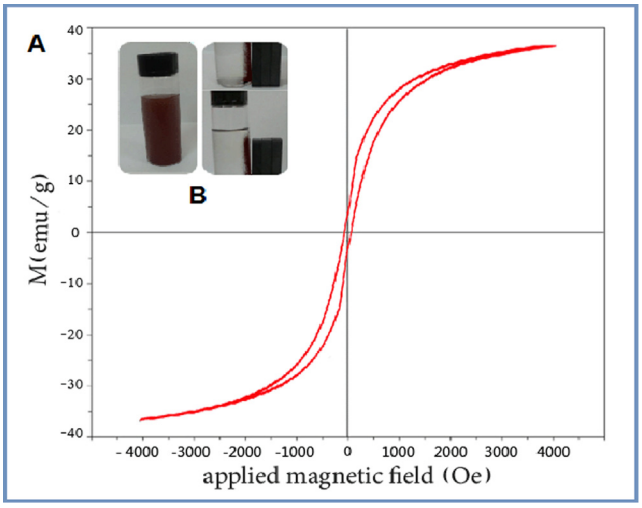

Fig. 12 (A) Magnetic hysteresis loops of Fe@AuNPs, (B) Image of the magnetic nanoparticles.

tion. The above compounds were evaluated for its antifungal activity against conidia's germination of *Alternaria tenuissima* Wiltshire, that cause pigeon pea leaf blight disease (Cajanuscajan) and these compounds were also used to control the pigeon pea Alternaria blight disease (Akintelu et al., 2021). The hydroxyl groups pattern of flavonoids is (myricetin > luteolin > quercetin > kaempferol) more hydroxyl groups lead to potent antibacterial activity against antibiotic resistant bacteria. The extract of (OLC) is changing the extracellular surface tension and thus leads to the lysis of bacterial cell membrane. Additionally, lipophilic flavonoids could also interrupt microbial membranes. Mechanism of antibacterial and antifungal activity of aqueous and organic extracts of the (OLC) extract and Fe@AuNPs possibly due to their ability to form a complex with bacterial cell walls and extracellular soluble proteins and that is lead to damage of microbial membranes then causing killing microbial cells. Some of the organic complexes of Au (I & III) and Fe (II & III) ions are antibacterial in nature. Fe@AuNPs are antifungal, but with conflicting results on their antibacterial activity (Inbaraj et al., 2020; Sathiyanarayanan et al., 2017). Results are shown in Fig. 14.

3.10.4. Anti-ulcer (ulcer-preventive) activity of Fe@AuNPs with (OLC) extract

3.10.4.1. Chemicals and reference drug: analytical grade chemicals were used in the current study. The triple regimen consisting of (Clarithromycin + Amoxicillin + Omeprazole) (reference drug) inhibit acid production by inhibiting the

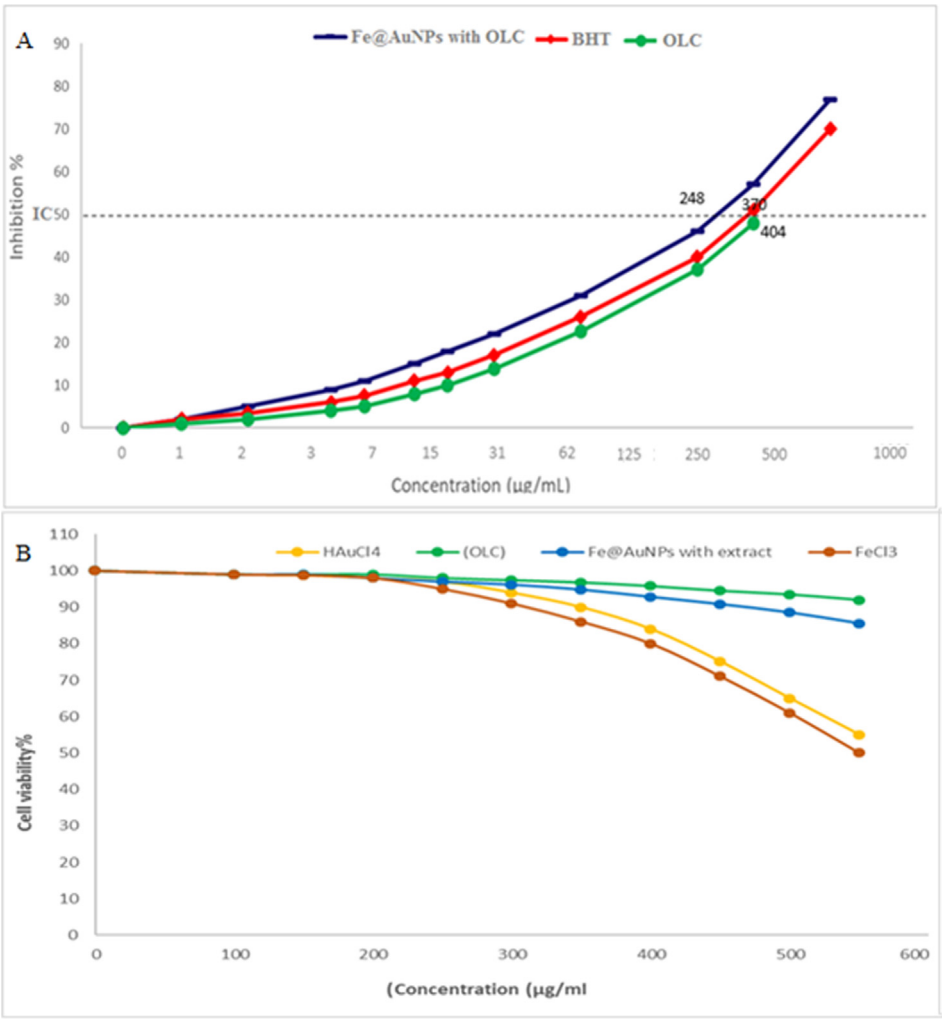

Fig. 13 (A) Antioxidant potential of Fe@AuNPs with extract, (OLC), and BHT (Butylated hydroxyltoluene) and (B)Percent viability measured on human umbilical vein endothelial cells after treatment with present Fe@AuNPs with extract, (OLC), $HAuCl_4$ and $FeCl_3$.

Table 7 Antibacterial activity of (OLC) extract and Fe@AuNPs.

Bacterial test strains	Mean diameter of inhibition zone (mm)/minimum inhibitory concentration (MIC) (µg/ml).					
	(OLC) extract		Fe@AuNPs		Norfloxacin (standard)	
	Inhibition zone	MIC	Inhibition zone	MIC	Inhibition zone	MIC
Bacillus subtilis (ATCC 6633)	22 ± 0.22	15.62 ± 0.05	28 ± 0.32	6.56 ± 0.26	24 ± 0.56	3.9 ± 0.12
Staphylococcus aureus (ATCC 29213)	24 ± 0.01	31.25 ± 0.45	29 ± 0.51	3.9 ± 0.55	23 ± 0.5	2.5 ± 0.35
Escherichia coli (ATCC 25922)	30 ± 0.32	7.51 ± 0.77	32 ± 0.01	1.95 ± 0.46	27 ± 0.98	1.57 ± 0.69
Pseudomonas aeruginosa (ATCC 27853)	25 ± 0.45	15.62 ± 0.02	28 ± 0.12	2.5 ± 0.87	25 ± 0.87	3.9 ± 0.47
Salmonella typhi (ATCC 6539)	27 ± 0.34	3.9 ± 0.08	29 ± 0.52	0.03 ± 0.14	23 ± 0.16	1.57 ± 0.25

enzymes in stomach wall and thus allowing the stomach to heal quickly.

3.10.4.2. Plant material and extract preparation. 2 g of licorice root is boiled in de-ionized water and 2 ml was taken from it, 2 ml of stock of olive oil and 1 ml of stock of coconut oil. Extract was taken and dissolved in 10 ml of PBS, 1% tween 80 was also used to make the extract properly dissolved in extract.

3.10.4.3. Animals. 91 Wistar rats (180–200 g) and male albino mice (20–25 g) was purchased and kept in ideal environment

Table 8 Antifungal activity of (OLC) extract and Fe@AuNPs.

Fungal test strains	Mean diameter of inhibition zone (mm)/ minimum inhibitory concentration (MIC) (μg/ml)					
	(OLC) extract		Fe@AuNPs		Nystatin (standard)	
	Inhibition zone	MIC	Inhibition zone	MIC	Inhibition zone	MIC
Candida albicans (ATCC 10231)	14 ± 0.34	31.25 ± 0.16	18 ± 0.56	6.56 ± 0.41	15 ± 0.2	7.81 ± 0.16
Aspergillus niger (RCMB 002007)	16 ± 0.23	15.62 ± 0.33	21 ± 0.61	13.5 ± 0.85	18 ± 0.2	20.5 ± 0.52
Aspergillus flavus (ATCC 16883)	19 ± 0.52	41.6 ± 0.26	20 ± 0.71	26.75 ± 0.56	17 ± 0.12	31.25 ± 0.45
Fusarium oxysporum (RCMB 008002)	18 ± 0.34	62.5 ± 0.75	22 ± 0.45	31.25 ± 0.55	20 ± 0.32	26.4 ± 0.2
Penicillium citrinum (RCMB 001011)	17 ± 0.16	31.25 ± 0.35	23 ± 0.81	29.75 ± 0.41	20 ± 0.20	31.25 ± 0.15

with supplement of rodent diet. CPCSEA guidelines were followed during experiments and the study was approved by Institutional animal ethical committee.

3.10.4.4. Acute toxicity study. Seven groups of albino mice's (13 in each group) were exposed to acute toxicity study of OLC extract. All the mice's were fasted overnight and admin-

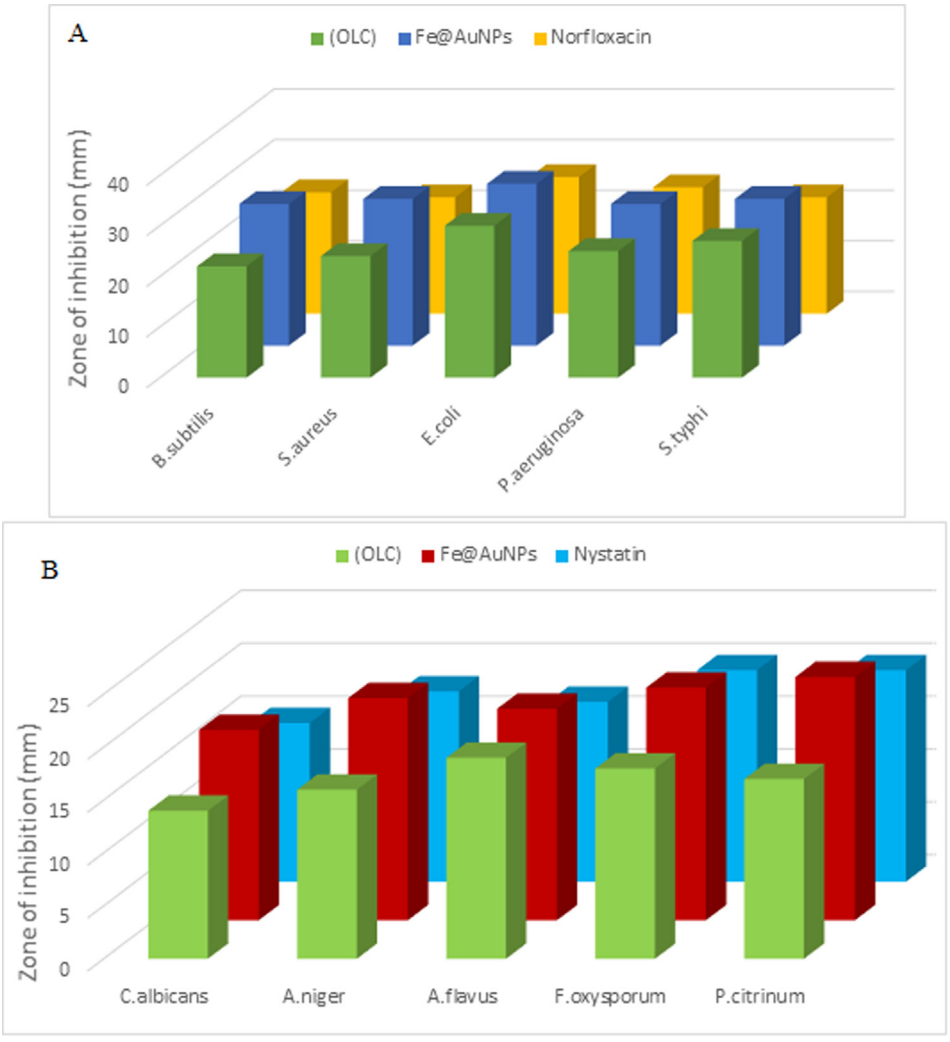

Fig. 14 (A) Antibacterial activity of (OLC) extract and Fe@AuNPs and (B)Antifungal activity of (OLC) extract and Fe@AuNPs.

istered with the OLC-Fe@AuNPs single dose of Conc. of 250, 500, 2000 and 5000 mg·kg^{-1}. Mice's were served with PBS as a control.

3.10.4.5. Anti-ulcer (ulcer-preventive) activity study. As stated in Table 9, treatment of Wister rats with OLC-Fe@AuNPs protect the stomach mucosal layer from ethanol induced ulcer.

Table 9 Anti-ulcer activity of omeprazole, OLC-Fe@AuNPs and (OLC) extract.

Treatment	Dose (mg/kg^{-1})	Ulcer area (mm^2)	Protection (%)
Control	NA	0.00 ± 0.0	NA
Ulcer control	0	891.00 ± 4.05	0.0
Drug control (Clarithromycin + Omeprazole + Amoxicillin)	8	211.03 ± 11.60	76.31%
Treatment 1 (OLC) extract	250 Low	596.35 ± 8.07	33.06%
Treatment 2 (OLC) extract	500 High	307.8 ± 6.29	65.45%
Treatment 3 (OLC-Fe@AuNPs)	250 Low	174.9 ± 12.043	80.37%
Treatment 4 (OLC-Fe@AuNPs)	500 High	14.6 ± 9.10	98.36%

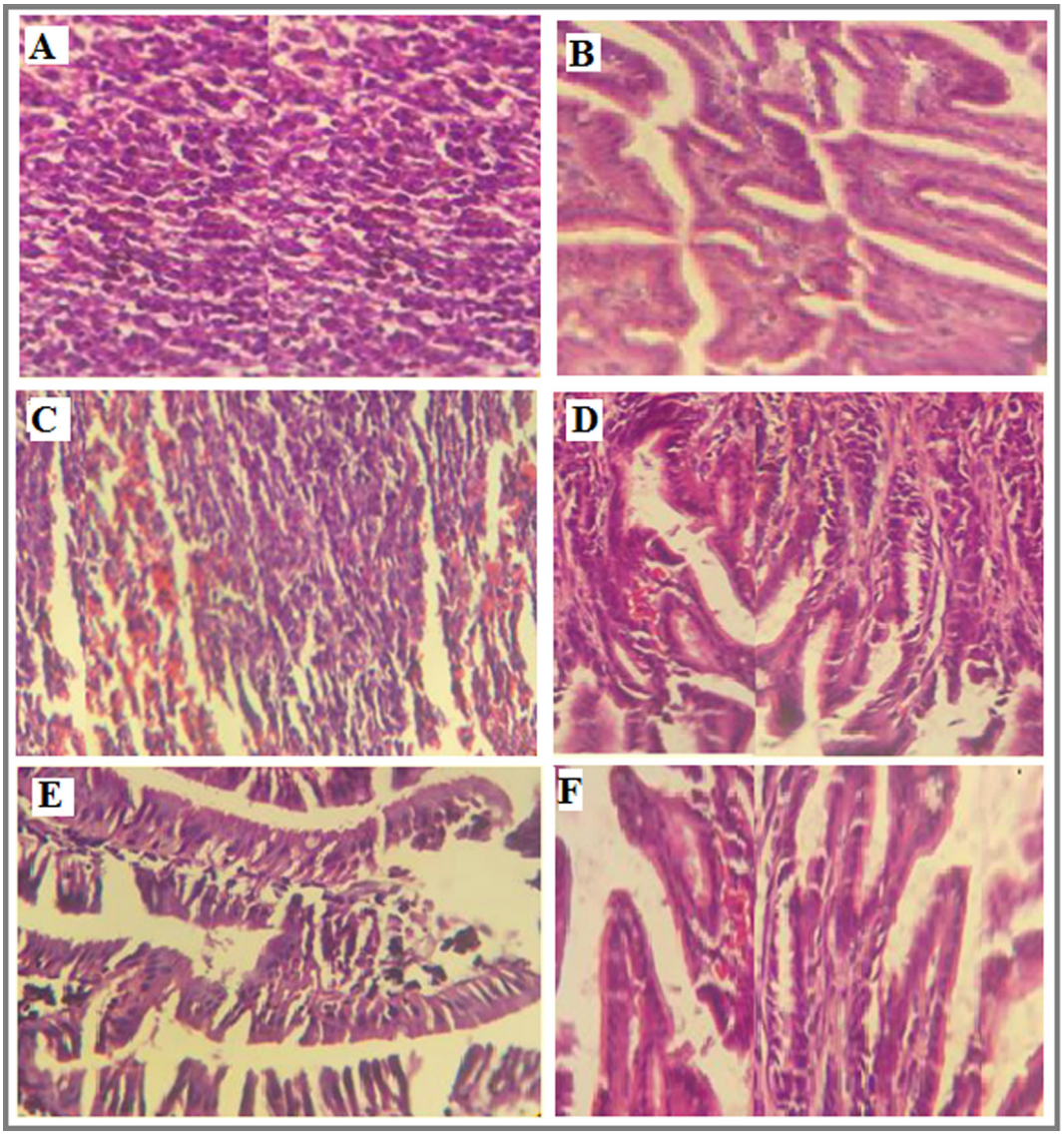

Fig. 15 Anti-ulcer activity of: (A) stomach of an ulcer control rat, (B) stomach of a rat treated with the reference drug, (C) stomach of a rat treated with 250 mg kg^{-1} (OLC) extract, (D) stomach of a rat treated with 500 mg kg^{-1} (OLC) extract, (E) stomach of a rat treated with 250 mg kg^{-1} OLC-Fe@AuNPs, (F) stomach of a rat treated with 500 mg kg^{-1} OLC-Fe@AuNPs.

OLC-Fe@AuNPs treatment protect the mucosal layer up to 80.37% and 98.36% respectively at 250 and 500 mg·kg^{-1} doses as compared to control groups. While the reference drug (Clarithromycin + omeprazole + amoxicillin) provided ulcer protection up to 76.31%. Samples without treatment of OLC-Fe@AuNPs showed complete ulceration Fig. 15A. Rats treated with reference drug showed protection as shown in Fig. 15B, 250, 500 mg·kg^{-1} (OLC) extract Fig. 15C, Fig. 15D and 250, 500 mg·kg^{-1} OLC-Fe@AuNPs Fig. 15E, Fig. 15F. Rats received almost 250 mg·kg^{-1} of OLC-Fe@AuNPs and significantly reduced gastric lesion formation and submucosal edema similar to the reference drug treated animals but the higher dose of 500 mg·kg^{-1} was much better, revealed from histopathological studies (Spósito, et al., 2019). OLC-Fe@AuNPs have various potential biomedical properties such as anti-inflammatory and anticancer. OLC-Fe@AuNPs mediated anti-ulcer activity was reported for the first time in the current study. The significant anti-ulcerative properties as shown in Table 9 revealed that OLC-Fe@AuNPs is gastro protective in nature and it was confirmed by histopathological studies. As antioxidant activities of the compounds, present in the extract may depend on structural features, such as the number of phenolic hydroxyl or methoxy groups and flavones hydroxyl as in Fig. 13A have been identified in the OLC-Fe@AuNPs, the anti-ulcer activity is due to the antioxidant nature of the extract as in Table 10. OLC-Fe@AuNPs is biocompatible as it is confirmed from sub-acute studies.

The final part of this study measured direct effects of OLC-Fe@AuNPs, (OLC) extract, olive oil, licorice root extract and coconut oil of levels of anti-*H. pylori*. Results given in Fig. 16 showed that all samples increased production of specific antibodies, supporting the hypothesis that (OLC) extract has strong anti-inflammatory and anticancer properties. In samples, OLC-Fe@AuNPs and OLC extract are showing the strongest affects followed by olive oil and licorice root extract with a medium difference, while coconut oil was the lowest one among them (Vetvicka et al., 2016).

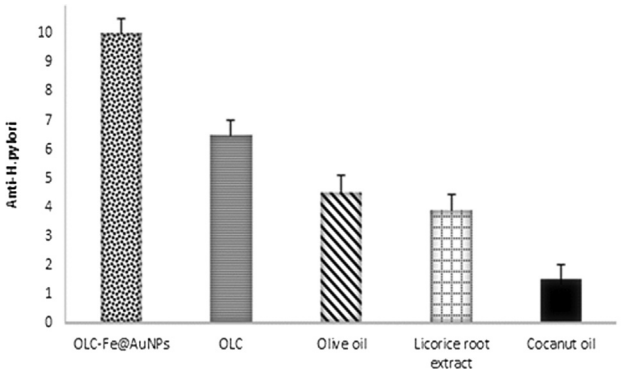

Fig. 16 Effects of OLC-Fe@AuNPs, (OLC) extract, olive oil, licorice root extract and coconut oil on anti-H.pylori.

4. Conclusion

It was concluded that using OLC extract as a capping g and reducing agent is a good choice for the synthesis of the Fe@AuNPs core–shell nanoparticles. Extracts of olive oil, licorice root extract and coconut oil have potent antimicrobial activities. It was also concluded that microwaves, temperature and pH optimization help to achieve the small sized nanoparticles that to be used in the therapeutics. The biosynthesized nanoparticles were characterized and confirmed by UV–Visible spectroscopy, Energy dispersive X-ray spectroscopy (EDX), X-ray diffraction (XRD), High resolution Transmission electron microscope (HR-TEM), Fourier Transform Infrared Spectroscopy (FT-IR) and high-performance liquid chromatography (HPLC), High angle annular dark-field scanning TEM (HAADF-STEM), Particle-Size Distribution (PSD), Magnetic hysteresis loops. *Helicobacter pylori* was successfully eradicated by iron coated gold nanoparticles and iron coated gold nanoparticles can be used as a therapeutic in stomach ulcer. The anti *H pylori* and anti-ulcer potential of biosynthesized nanoparticles were checked *in vivo* in animal

Table 10 Changes in the animal behavior after administration of OLC-Fe@AuNPs 5000 mg kg^{-1} dose.

Time after administration (h)						
Gross activity	2	3	5	7	12	24
Respiration	–	–	–	–	–	–
Writhing	–	–	–	–	–	–
Tremors	–	–	–	–	–	–
Convulsion	–	–	–	–	–	–
Salivation	–	–	–	–	–	–
Diarrhea	–	–	–	–	–	–
Mortality	–	–	–	–	–	–
Hind limb paralysis	–	–	–	–	–	–
Sedation	–	–	–	–	–	–
Skin irritation	–	–	–	–	–	–
Eye irritation	–	–	–	–	–	–
CNS Depression	–	–	–	–	–	–

+: Indicates that change was observed; –: Indicates that there was no change.

model (Wister rats). The antimicrobial properties revealed that nanoparticles encounter with bacterial cell membrane and leads to its damage and thus proved itself a good option to be considered as an antimicrobial. The OLC mediated Fe@Au nanoparticles were found nontoxic at high concentration but proper cytotoxic studies are recommended to use nanoparticles *in vivo*.

Declaration of Competing Interest

The authors declare that they have no known competing financial interests or personal relationships that could have appeared to influence the work reported in this paper.

Acknowledgement

I would like to express my sincere thanks to Saudi Patent Office at (SAIPKSA) for providing adequate information and facilitate the registration of the patent number (7403), titled ''Microwave Assisted Green Synthesis of Fe@Au core-shell Nanoparticales Magnetic to Enhance Olive oil Efficiency on Eradication of Helicobacter Pylori'' in (24/12/2020).

Appendix A. Supplementary material

Supplementary data to this article can be found online at https://doi.org/10.1016/j.arabjc.2022.103685.

References

Abdullah, A.-R., Al-Radadi, N.S, Hussain, T, Faisal, S.S, Raza, S. A., 2022. Novel biosynthesis, characterization and bio-catalytic potential of green algae (Spirogyra hyalina) mediated silver nanomaterial's. Saudi J. Biol. Sci. 29 (1), 411–419. https://doi.org/10.1016/j.sjbs.2021.09.013.

Abdoli, M., Arkan, E., Shekarbeygi, Z., Khaledian, S., 2021. Green synthesis of gold nanoparticles using Centaurea behen leaf aqueous extract and investigating their antioxidant and cytotoxic effects on acute leukemia cancer cell line (THP-1). Inorg. Chem. Commun. 129, 108649. https://doi.org/10.1016/j.inoche.2021.108649.

Abou Baker, D., 2020. Plants against Helicobacter pylori to combat resistance: an ethnopharmacological review. Biotechnol. Rep, 26, e00470. https://doi.org/10.1016/j.btre.2020.e00470.

Adawiyah, R., Abu, F., Khairul, M., 2019. Elucidation of synergistic effect of eucalyptus globulus honey and Zingiber officinale in the synthesis of colloidal biogenic gold nanoparticles with antioxidant and catalytic properties. Sustain. Chem. Pharm. 13 (June), 100156. https://doi.org/10.1016/j.scp.2019.100156.

Ahmad, A., Syed, F., Shah, A., Khan, Z., Tahir, K., Khan, A.U., Yuan, Q., 2015. Silver and gold nanoparticles from Sargentodoxa cuneata: synthesis, characterization and antileishmanial activity. RSC Adv. 5 (90), 73793–73806.

Ahmed, S., Annu, Ikram, S., Yudha, S., 2016. Biosynthesis of gold nanoparticles: a green approach. J. Photochem. Photobiol. B: Biol. 161, 141–153. https://doi.org/10.1016/j.jphotobiol.2016.04.034.

Akintelu, S.A., Yao, B., Folorunso, A.S., 2021. Green synthesis, characterization, and antibacterial investigation of synthesized gold nanoparticles (AuNPs) from Garcinia kola pulp extract. Plasmonics 16 (1), 157–165. https://doi.org/10.1007/s11468-020-01274-9.

Al-Radadi, N.S., 2018. Artichoke (Cynara scolymus L.), mediated rapid analysis of silver nanoparticles and their utilisation on the cancer cell treatments. J. Comput. Theor. Nanosci. 15 (6–7), 1818–1829. https://doi.org/10.1166/jctn.2018.7317.

Al-Radadi, N.S., 2019. Green synthesis of platinum nanoparticles using Saudi's Dates extract and their usage on the cancer cell treatment. Arab. J. Chem. 12 (3), 330–349. https://doi.org/10.1016/j.arabjc.2018.05.008.

Al-Radadi, N.S., Adam, S.I.Y., 2020. Green biosynthesis of Pt-nanoparticles from Anbara fruits: toxic and protective effects on CCl4 induced hepatotoxicity in Wister rats. Arab. J. Chem. 13 (2), 4386–4403. https://doi.org/10.1016/j.arabjc.2019.08.008.

Al-Radadi, N.S., Al-Youbi, A.N., 2018a. One-step synthesis of au nano-assemblies and study of their anticancer activities. J. Comput. Theor. Nanosci. 15 (6–7), 1861–1870. https://doi.org/10.1166/jctn.2018.7323.

Al-Radadi, N.S., Al-Youbi, A.N., 2018b. Environmentally-safe synthesis of gold and silver nano-particles with AL-Madinah Barni fruit and their applications in the cancer cell treatments. J. Comput. Theor. Nanosci. 15 (6–7), 1853–1860. https://doi.org/10.1166/jctn.2018.7322.

Al-Radadi, N.S., 2021a. Facile one-step green synthesis of gold nanoparticles (AuNp) using Licorice root extract: antimicrobial and anticancer study against HepG2 cell line. Arab. J. Chem. 14. https://doi.org/10.1016/j.arabjc.2020.102956.

Al-Radadi, N.S., 2021-b. Green biosynthesis of flaxseed gold nanoparticles (Au-NPs) as potent anticancer agent against breast cancer cells. J. Saudi. Chem. Soc. 25 (6). https://doi.org/10.1016/j.jscs.2021.101243.

Al-Radadi, N.S., 2022. Biogenic proficient synthesis of (Au-NPs) via aqueous extract of red dragon pulp and seed oil: characterization, antioxidant, cytotoxic properties, anti-diabetic antiinflammatory, anti-alzheimer and their anti -proliferative potential against cancer cell lines. Saudi J. Biol. Sci. https://doi.org/10.1016/j.sjbs.2022.01.001.

Alam, M.N., Das, S., Batuta, S., Mandal, D., Begum, N.A., 2016. Green-nanochemistry for safe environment: bio-friendly synthesis of fluorescent monometallic (Ag and Au) and bimetallic (Ag/Au alloy) nanoparticles having pesticide sensing activity. J. Nanostruct. Chem. 6 (4), 373–395. https://doi.org/10.1007/s40097-016-0209-y.

Aminde, J.A., Dedino, G.A., Ngwasiri, C.A., Ombaku, K.S., Makon, C.A.M., Aminde, L.N., 2019. Helicobacter pylori infection among patients presenting with dyspepsia at a primary care setting in Cameroon: seroprevalence, five-year trend and predictors. BMC Infect. Dis. 19 (30), 1–9. https://doi.org/10.1186/s12879-019-3677-0.

Anjana, P.M., Bindhu, M.R., Rakhi, R.B., 2019. Green synthesized gold nanoparticle dispersed porous carbon composites for electrochemical energy storage. Mater. Sci. Technol. 2 (3), 389–395. https://doi.org/10.1016/j.mset.2019.03.006.

Baltas, N., Karaoglu, S.A., Tarakci, C., Kolayli, S., 2016. Effect of propolis in gastric disorders: inhibition studies on the growth of Helicobacter pylori and production of its urease. J. Enzyme Inhib. Med. Chem. 31, 46–50. https://doi.org/10.1080/14756366.2016.1186023.

Ban, Z., Barnakov, Y.A., Li, F., Golub, V.O., O'Connor, C.J., 2005. The synthesis of core-shell iron@gold nanoparticles and their characterization. J. Mater. Chem. 15 (43), 4660–4662. https://doi.org/10.1039/b504304b.

Bandyopadhyay, S., Singh, G., Sandvig, I., Sandvig, A., Mathieu, R., Kumar, P.A., Robert, W., 2014. Applied Surface Science Synthesis and in vitro cellular interactions of superparamagnetic iron nanoparticles with a crystalline gold shell. Appl. Surf. Sci. 316, 171–178. https://doi.org/10.1016/j.apsusc.2014.07.081.

Benites, J., Toledo, H., Salas, F., Guerrero, A., Rios, D., Valderrama, J.A., Calderon, P.B., 2018. In vitro inhibition of helicobacter pylori growth by redox cycling phenylaminojuglones. Oxid. Med. Cell. Longevity 1–9. https://doi.org/10.1155/2018/1618051.

Boyanova, L., Derejian, S., Koumanova, G., Mitov, L., Nikolov, R., Kraste, Z., 2003. Inhibition of Helicobacter pylori growth in vitro

by Bulgarian propolis: preliminary report. J. Med. Microbiol. 52, 417–419. https://doi.org/10.1099/jmm.0.04895-0.

Carroll, K.J., Hudgins, D.M., Spurgeon, S., Kemner, K.M., Mishra, B., Boyanov, M.I., Brown, L.W., Taheri, M.L., Carpenter, E.E., 2010. One-pot aqueous synthesis of Fe and Ag core/shell nanoparticles. Chem. Mater. 22 (23), 6291–6296. https://doi.org/10.1021/cm101996u.

Chahardoli, A., Karimi, N., Sadeghi, F., Fattahi, A., 2018. Green approach for synthesis of gold nanoparticles from Nigella arvensis leaf extract and evaluation of their antibacterial, antioxidant, cytotoxicity and catalytic activities. Artif. Cells Nanomed. Biotechnol. 46 (3), 579–588. https://doi.org/10.1080/21691401.2017.1332634.

Chen, H.C., Liu, Y.C., 2018. Creating functional water by treating excited gold nanoparticles for the applications of green chemistry, energy and medicine: a review. J. Ind. Eng. Chem. 60, 9–18. https://doi.org/10.1016/j.jiec.2017.09.026.

Chen, J., Li, Y., Fang, G., Cao, Z., Shang, Y., Alfarraj, S., Alharbi, S.A., Li, J., Yang, S., Duan, X., 2021. Green synthesis, characterization, cytotoxicity, antioxidant, and anti-human ovarian cancer activities of Curcumae kwangsiensis leaf aqueous extract green-synthesized gold nanoparticles. Arab. J. Chem. 14 (3), 103000.

Chen, C., Mao, Y., Du, J., Xu, Y., Zhu, Z., Khairul, M., Cao, H., 2019a. Helicobacter pylori infection associated with an increased risk of colorectal adenomatous polyps in the Chinese population. BMC Gastroenterol. 19 (14), 1–6. https://doi.org/10.1186/s12876-018-0918-4.

Chen, Y., Yuan, P.X., Wang, A.J., Luo, X., Xue, Y., Zhang, L., Feng, J.J., 2019b. A novel electrochemical immunosensor for highly sensitive detection of prostate-specific antigen using 3D open-structured PtCu nanoframes for signal amplification. Biosens. Bioelectron. 126 (October 2018), 187–192. https://doi.org/10.1016/j.bios.2018.10.057.

Choi, C.W., Kim, S.C., Hwang, S.S., Choi, B.K., Ahn, H.J., Lee, M. Y., Kim, S.K., 2002. Antioxidant activity and free radical scavenging capacity between Korean medicinal plants and flavonoids by assay-guided comparison. Plant Sci. 163 (6), 1161–1168. https://doi.org/10.1016/S0168-9452(02)00332-1.

Chung, R.J., Shih, H.T., 2014. Preparation of multifunctional Fe@Au core-shell nanoparticles with surface grafting as a potential treatment for magnetic hyperthermia. Materials 7 (2), 653–661. https://doi.org/10.3390/ma7020653.

Collares-Pelizaro, R.V.A., Santos, J.S., Nonino, C.B., Gaitani, C.M., Jr, W.S., 2017. Omeprazole absorption and fasting Gastrinemia after Roux-en-Y gastric bypass. Obes. Surg. 27, 2303–2307. https://doi.org/10.1007/s11695-017-2672-z.

Dayrit, F.M., 2014. The properties of lauric acid and their significance in coconut oil. J. Am. Oil Chem. Soc. 92 (1), 1–15. https://doi.org/10.1007/s11746-014-2562-7.

Devi, G.K., Suruthi, P., Veerakumar, R., Vinoth, S., Subbaiya, R., Chozhavendhan, S., 2019. A review on metallic gold and silver nanoparticles. Res. J. Pharm. Technol. 12 (2), 935–943. https://doi.org/10.5958/0974-360X.2019.00158.6.

Díaz-Gómez, R., López-Solís, R., Obreque-Slier, E., Toledo-Araya, H., 2013. Comparative antibacterial effect of gallic acid and catechin against Helicobacter pylori. LWT – Food Sci. Technol. 54, 331e335. https://doi.org/10.1016/j.lwt.2013.07.012.

Di Pierro, F., Bertuccioli, A., Saponara, M., Ivaldi, L., 2020. Impact of a two-bacterial-strain formula, containing Bifidobacterium animalis lactis BB-12 and Enterococcus faecium L3, administered before and after therapy for Helicobacter pylori eradication. Minerva Gastroenterol. Dietol. 66 (2), 100156.

El-Naggar, M.E., Shaheen, T.I., Fouda, M.M.G., Hebeish, A.A., 2016. Eco-friendly microwave-assisted green and rapid synthesis of well-stabilized gold and core-shell silver-gold nanoparticles. Carbohydr. Polym. 136, 1128–1136. https://doi.org/10.1016/j.carbpol.2015.10.003.

El-Shouny, W.A., Ali, S.S., Hegazy, H.M., Abd Elnabi, M.K., Ali, A., Sun, J., 2020. Syzygium aromaticum L.: traditional herbal medicine against cagA and vacA toxin genes-producing drug resistant Helicobacter pylori. J. Tradit. Complement. Med. 10 (4), 366–377. https://doi.org/10.1016/j.jtcme.2019.05.002.

Etik, D.Ö., Sezer, S., Suna, N., Öztaş, E., Kiliç, Z.M.Y., 2019. Can the treatment duration be shortened in bismuth-containing therapies for Helicobacter pylori eradication? Turkish J. Gastroenterol. 30 (8), 667–672. https://doi.org/10.5152/tjg.2019.18793.

Farhadkhani, M., Nikaeen, M., Hassanzadeh, A., Nikmanesh, B., 2019. Potential transmission sources of Helicobacter pylori infection: detection of H. pylori in various environmental samples. J. Environ. Health Sci. Eng. 17 (1), 129–134. https://doi.org/10.1007/s40201-018-00333-y.

Fathi-Achachelouei, M., Knopf-Marques, H., Ribeiro da Silva, C.E., Barthès, J., Bat, E., Tezcaner, A., Vrana, N.E., 2019. Use of nanoparticles in tissue engineering and regenerative medicine. Front. Bioeng. Biotechnol. 7 (May), 1–22. https://doi.org/10.3389/fbioe.2019.00113.

Faisal, S., Al-Radadi, N.S., Jan, H., Shah, S.A., Shah, S., Rizwan, M., Afsheen, Z., Hussain, Z., Uddin, M.N., Idrees, M., Bibi, N., 2021. Curcuma longa mediated synthesis of copper oxide, nickel oxide and Cu-Ni bimetallic hybrid nanoparticles: characterization and evaluation for antimicrobial, anti-parasitic and cytotoxic potentials. Coatings 11, 1–23. https://doi.org/10.3390/coatings11070849.

Fagoonee, S., Pellicano, R., 2019. Helicobacter pylori: molecular basis for colonization and survival in gastric environment and resistance to antibiotics. A short review. Infectious Diseases 51 (6), 399–408. https://doi.org/10.1080/23744235.2019.1588472.

Foscolou, A., Critselis, E., Panagiotakos, D., 2018. Olive oil consumption and human health: a narrative review. Maturitas 118 (October), 60–66. https://doi.org/10.1016/j.maturitas.2018.10.013.

Francis, S., Koshy, E.P., Mathew, B., 2018. Green synthesis of Stereospermum suaveolens capped silver and gold nanoparticles and assessment of their innate antioxidant, antimicrobial and antiproliferative activities. Bioprocess Biosyst. Eng. https://doi.org/10.1007/s00449-018-1925-0.

Gawande, M., Goswami, A., Asefa, T., Guo, H., Biradar, A.V., Peng, D.-L., Zboril, R., Rajender, V.S., 2015. Core – shell nanoparticles: synthesis and applications in catalysis and electrocatalysis. Chem. Soc. Rev. 44, 7540–7590. https://doi.org/10.1039/C5CS00343A.

Ghani, N.A.A., Channip, A.A., Chok Hwee Hwa, P., Ja'afar, F., Yasin, H.M., Usman, A., 2018. Physicochemical properties, antioxidant capacities, and metal contents of virgin coconut oil produced by wet and dry processes. Food Sci. Nutrit. 6 (5), 1298–1306. https://doi.org/10.1002/fsn3.671.

Ghormade, V., Deshpande, M.V., Paknikar, K.M., 2011. Perspectives for nano-biotechnology enabled protection and nutrition of plants. Biotechnol. Adv. 29 (6), 792–803. https://doi.org/10.1016/j.biotechadv.2011.06.007.

Gorzynik-Debicka, M., Przychodzen, P., Cappello, F., Kuban-Jankowska, A., Gammazza, A.M., Knap, N., Wozniak, M., Gorska-Ponikowska, M., 2018. Potential health benefits of olive oil and plant polyphenols. Int. J. Mol. Sci. 19 (3). https://doi.org/10.3390/ijms19030686.

Haghighi, M.B., Dara, N., Ghanaie, R.M., Azimi, L., Hosseini, A., Tajalli, S., Hajipour, M., Sayyari, A., Imanzadeh, F., Khatami, K., Rohani, P., Olang, B., 2019. Evaluation of clarithromycin and metronidazole resistance of helicobacter pylori infection in symptomatic Iranian children. Int. J. Pediatrics-Mashhad 7 (2), 8925–8933. https://doi.org/10.22038/ijp.2018.34347.3028.

Hosny, M., Fawzy, M., 2021. Instantaneous phytosynthesis of gold nanoparticles via Persicaria salicifolia leaf extract, and their medical applications. Adv. Powder Technol. 32 (8), 2891–2904. https://doi.org/10.1016/j.apt.2021.06.004.

Rodríguez-León, E., Rodríguez-Vázquez, B.E., Martínez-Higuera, A., Rodríguez-Beas, C., Larios-Rodríguez, E., Navarro, R.E., López-Esparza, R., Iñiguez-Palomares, R.A., 2019. Synthesis of Gold Nanoparticles Using Mimosa tenuiflora Extract, Assessments of Cytotoxicity, Cellular Uptake, and Catalysis. Rodríguez-León et al. Nanoscale Research Letters 14, 334. https://doi.org/10.1186/s11671-019-3158-9.

Hajiaghamohammadi, A.A., Zargar, A., Oveisi, S., Samimi, R., Reisian, S., 2016. To evaluate of the effect of adding licorice to the standard treatment regimen of Helicobacter pylori. Brazil. J. Infect. Dis. 20 (6), 534–538. https://doi.org/10.1016/j.bjid.2016.07.015.

Hassan, D.F., Mahmood, M.B., 2019. Biosynthesis of iron oxide nanoparticles using Escherichia coli. Iraqi J. Sci. 60 (3), 453–459. https://doi.org/10.24996/ijs.2019.60.3.5.

Hien Pham, T.T., Cao, C., Sim, S.J., 2008. Application of citrate-stabilized gold-coated ferric oxide composite nanoparticles for biological separations. J. Magn. Magn. Mater. 320 (15), 2049–2055. https://doi.org/10.1016/j.jmmm.2008.03.015.

Hosseynizadeh Khezri, S., Yazdani, A., Khordad, R., 2012. Pure iron nanoparticles prepared by electric arc discharge method in ethylene glycol. EPJ Appl. Phys. 59 (3). https://doi.org/10.1051/epjap/2012110303.

Inbaraj, B.S., Chen, B.Y., Liao, C.W., Chen, B.H., 2020. Green synthesis, characterization and evaluation of catalytic and antibacterial activities of chitosan, glycol chitosan and poly(γ-glutamic acid) capped gold nanoparticles. Int. J. Biol. Macromol. 161, 1484–1495. https://doi.org/10.1016/j.ijbiomac.2020.07.244.

Ionescu, A.M., 2016. Nanotechnology and global security. Connect.: Quart. J. 15 (2), 31–47. https://doi.org/10.11610/connections.15.2.03.

Isaeva, G., Isaeva, R., 2020. Molecular methods for the detection of Helicobacter pylori. Minerva Biotecnologica 32 (4), 182–187. https://doi.org/10.23736/S1120-4826.20.02665-8.

Jeevanandam, J., Barhoum, A., Chan, Y.S., Dufresne, A., Danquah, M.K., 2018. Review on nanoparticles and nanostructured materials: history, sources, toxicity and regulations. Beilstein J. Nanotechnol. 9 (1), 1050–1074. https://doi.org/10.3762/bjnano.9.98.

Karkanis, A., Martins, N., Petropoulos, S.A., Ferreira, I.C.F.R., 2018. Phytochemical composition, health effects, and crop management of liquorice (Glycyrrhiza glabra L.): a medicinal plant. Food Rev. Int. 34 (2), 182–203. https://doi.org/10.1080/87559129.2016.1261300.

Karthik, R., Govindasamy, M., Chen, S.M., Mani, V., Lou, B.S., Devasenathipathy, R., Hou, Y.S., Elangovan, A., 2016. Green synthesized gold nanoparticles decorated graphene oxide for sensitive determination of chloramphenicol in milk, powdered milk, honey and eye drops. J. Colloid Interface Sci. 475, 46–56. https://doi.org/10.1016/j.jcis.2016.04.044.

Saravanakumar, K., Sathiyaseelan, A., Mariadoss, A.V.A., Hu, X., Venkatachalam, K., Wang, M.H., 2021. Nucleolin targeted delivery of aptamer tagged Trichoderma derived crude protein coated gold nanoparticles for improved cytotoxicity in cancer cells. Process Biochem., 325–332 https://doi.org/10.1016/j.procbio.2021.01.022.

Khan, I., Saeed, K., Khan, I., 2019a. Nanoparticles: properties, applications and toxicities. Arab. J. Chem. 12 (7), 908–931. https://doi.org/10.1016/j.arabjc.2017.05.011.

Khan, M.J., Shameli, K., Sazili, A.Q., Selamat, J., Kumari, S., 2019b. Rapid green synthesis and characterization of silver nanoparticles arbitrated by curcumin in an alkaline medium. Molecules 24 (4). https://doi.org/10.3390/molecules24040719.

Khan, Z.U.H., Khan, A., Chen, Y., Shah, N.S., Muhammad, N., Khan, A.U., Tahir, K., Khan, F.U., Murtaza, B., Hassan, S.U., Qaisrani, S.A., Wan, P., 2017. Biomedical applications of green synthesized Nobel metal nanoparticles. J. Photochem. Photobiol., B 173 (May), 150–164. https://doi.org/10.1016/j.jphotobiol.2017.05.034.

Koletzko, L., Macke, L., Schulz, C., Malfertheiner, P., 2019. Helicobacter pylori eradication in dyspepsia: new evidence for symptomatic benefit. Best Pract. Res. Clin. Gastroenterol. 40–41, 101637. https://doi.org/10.1016/j.bpg.2019.101637.

Kumar, B., Smita, K., Debut, A., Cumbal, L., 2018. Environmental Nanotechnology, Monitoring & Management Utilization of Persea americana (Avocado) oil for the synthesis of gold nanoparticles in sunlight and evaluation of antioxidant and photocatalytic activities. Environ. Nanotechnol. Monit. Manage. 10 (July), 231–237. https://doi.org/10.1016/j.enmm.2018.07.009.

Kumar, B., Smita, K., Borovskikh, P., Shchegolkov, A., Debutb, A., Cumbal, L., 2021. Spectroscopic and morphological characterization of Nephelium lappaceum peel extract synthesized gold nanoflowers and its catalytic activity. Inorgan. Chem. Commun. 133. https://doi.org/10.1016/j.inoche.2021.108868.

Kurauchi, Y., Devkota, H.P., Hori, K., Nishihara, Y., Hisatsune, A., Seki, T., Katsuki, H., 2019. Anxiolytic activities of Matcha tea powder, extracts, and fractions in mice: contribution of dopamine D1 receptor- and serotonin 5-HT1A receptor-mediated mechanisms. J. Funct. Foods 59, 301–308. https://doi.org/10.1016/j.jff.2019.05.046.

Kumar, S., Nehra, M., Dilbaghi, N., Marrazza, G., Hassan, A.A., Kim, K.H., 2019a. Nano-based smart pesticide formulations: emerging opportunities for agriculture. J. Controll. Release 294, 131–153. https://doi.org/10.1016/j.jconrel.2018.12.012.

Kvitek, O., Reznickova, A., Zelenakova, A., Zelenak, V., Orendac, M., Svorcik, V., 2019. Immobilization of Fe @ Au superparamagnetic nanoparticles on polyethylene. Eur. Polym. J. 110 (July 2018), 56–62. https://doi.org/10.1016/j.eurpolymj.2018.10.043.

Lakhiar, J.A., Khan, M.A., Akash, A., Imran, M., Raza, M.H., 2018. Helicobacter pylori: a clinical review. J. Med. Physiol. Biophys. 47, 22–25.

Leja, M., Axon, A., Brenner, H., 2016. Epidemiology of Helicobacter pylori infection. Helicobacter 21, 3–7. https://doi.org/10.1111/hel.12332.

Li, Y., Zhu, X., Weiss, P.S., 2018. Nanoscience and nanotechnology research at Peking University. ACS Nano 12 (5), 4075–4076. https://doi.org/10.1021/acsnano.8b02778.

Liu, D., Hong, Y., Li, Y., Hu, C., Yip, T.C., Yu, W.K., Zhu, Y., Fong, C.C., Wang, W., Au, S.K., Wang, S., Yang, M., 2020. Targeted destruction of cancer stem cells using multifunctional magnetic nanoparticles that enable combined hyperthermia and chemotherapy. Theranostics 10 (3), 1181–1196. https://doi.org/10.7150/thno.38989.

Lombardo, D., Kiselev, M.A., Caccamo, M.T., 2019. Smart nanoparticles for drug delivery application: development of versatile nanocarrier platforms in biotechnology and nanomedicine. J. Nanomater. 2019. https://doi.org/10.1155/2019/3702518.

Machado, S., Grosso, J.P., Nouws, H.P.A., Albergaria, J.T., Delerue-Matos, C., 2014. Utilization of food industry wastes for the production of zero-valent iron nanoparticles. Sci. Total Environ. 496, 233–240. https://doi.org/10.1016/j.scitotenv.2014.07.058.

Marina, A.M., Che Man, Y.B., Amin, I., 2009. Virgin coconut oil: emerging functional food oil. Trends Food Sci. Technol. 20 (10), 481–487. https://doi.org/10.1016/j.tifs.2009.06.003.

Martin, D.K., 2019. Low-frequency ultrasound can drive the transport of nanoparticles and molecules in polymer gels for biotechnology applications. EuroBiotech J. 3 (1), 1–9. https://doi.org/10.2478/ebtj-2019-0001.

Martínez-Prieto, L.M., Chaudret, B., 2018. Organometallic ruthenium nanoparticles: synthesis, surface chemistry, and insights into ligand coordination. Acc. Chem. Res. 51 (2), 376–384. https://doi.org/10.1021/acs.accounts.7b00378.

Menazea, A.A., Ismail, A.M., Samy, A., 2021. Novel green synthesis of zinc oxide nanoparticles using orange waste and its thermal and antibacterial activity. J. Inorg. Organomet. Polym Mater. 31, 4250–4259. https://doi.org/10.1007/s10904-021-02074-2.

Meng, J., Chen, T., Zhao, Y., Lu, S., Yu, H., Chang, Y., Chen, D., 2019. Study of the mechanism of anti-ulcer effects of virgin coconut oil on gastric ulcer-induced rat model. Sustain. Chem. Pharm. 15 (5), 1329–1335. https://doi.org/10.5114/aoms.2018.76943.

Melese, A., Abu, Genet, C., Zeleke, B., Andualem, T., 2019. Helicobacter pylori infections in Ethiopia; prevalence and associated factors: a systematic review and meta-analysis. BMC Gastroenterol. 19 (8), 1–15. https://doi.org/10.1186/s12876-018-0927-3.

Modolo, L.V., de Souza, A.X., Horta, L.P., Araujo, D.P., de Fátima, A., 2015. An overview on the potential of natural products as ureases inhibitors: a review. J. Adv. Res. 6, 35–44. https://doi.org/10.1016/j.jare.2014.09.001.

Mohammadi, H., Nekobahr, E., Akhtari, J., Saeedi, M., Akbari, J., Fathi, F., 2021. Synthesis and characterization of magnetite nanoparticles by co-precipitation method coated with biocompatible compounds and evaluation of in-vitro cytotoxicity. Toxicol. Rep. 8, 331–336. https://doi.org/10.1016/j.toxrep.2021.01.012.

Mooney, S., 2002. The use of mineral magnetic parameters to characterize archaeological ochres. J. Archaeol. Sci. https://doi.org/10.1006/jasc.2002.0856.

Murali, M.R., Naveen, S.V., Son, C.G., Raghavendran, H.R.B., 2014. ECurrent knowledge on alleviating Helicobacter pylori infections through the use of some commonly known natural products: bench to bedside. Integ. Med. Res. 3 (3), 111–118. https://doi.org/10.1016/j.imr.2014.04.001.

Muniyappan, N., Pandeeswaran, M., Amalraj, A., 2021. Green synthesis of gold nanoparticles using Curcuma pseudomontana isolated curcumin: its characterization, antimicrobial, antioxidant and anti- inflammatory activities. Environ. Chem. Ecotoxicol. 3, 117–124. https://doi.org/10.1016/j.enceco.2021.01.002.

Nafisi, S., and Maibach, H.I., 2017. Nanotechnology in cosmetics. In: Cosmetic Science and Technology: Theoretical Principles and Applications. https://doi.org/10.1016/B978-0-12-802005-0.00022-7.

Narayan, N., Meiyazhagan, A., Vajtai, R., 2019. Metal nanoparticles as green catalysts. Mater. IEEE Trans. Magn. 12 (21), 1–12. https://doi.org/10.3390/ma12213602.

Ngnameko, C.R., Njayou, F.N., Fowora, M., Nemg, F.B.S., Fewou, P.M., Smith, S.I., 2019. Inhibitory effect of medicinal plants from Cameroon on the growth and adhesion of Helicobacter pylori. Eur. J. Integ. Med. 30, 100957. https://doi.org/10.1016/j.eujim.2019.100957.

Obaidat, I.M., Issa, B., Haik, Y., 2014. Magnetic properties of magnetic nanoparticles for efficient hyperthermia. Nanomaterials 5 (1), 63–89. https://doi.org/10.3390/nano5010063.

Ofori, E.G., Adinortey, C.A., Bockarie, A.S., Kyei, F., Tagoe, E.A., Adinortey, M.B., 2019. Helicobacter pylori infection, virulence genes' distribution and accompanying clinical outcomes: the West Africa Situation. Biomed. Res. Int. 2019. https://doi.org/10.1155/2019/7312908.

Onifade, A.K., Bakare, M.A., 2019. Plasmid Analysis and Curing of Multidrug Resistant of Helicobacter pylori Isolated from Ulcer Patients in Ondo State, Nigeria. J. Adv. Microbiol. 16 (1), 1–8. https://doi.org/10.9734/jamb/2019/v16i130115.

Ovejero, J.G., Bran, C., Vilanova, E., Kosel, J., Morales, M.P., Vazquez, M., 2015. Electrochemical synthesis of core-shell magnetic nanowires. J. Magn. Magn. Mater. 389, 144–147. https://doi.org/10.1016/j.jmmm.2015.04.059.

Paciotti, G.F., Myer, L., Weinreich, D., Goia, D., Pavel, N., McLaughlin, R.E., Tamarkin, L., 2004. Colloidal gold: a novel nanoparticle vector for tumor directed drug delivery. Drug Deliv.: J. Deliv. Target. Therap. Agents 11 (3), 169–183. https://doi.org/10.1080/10717540490433895.

Padma, M., Govindh, B., Rao, B.V., 2014. Synthesis & characterization of fluorescent silver nanoparticles stabilized by Tinospora Cordifolia leaf extract-A green procedure. Int. J. Eng. Res. Appl. 4 (9), 100–107.

Pana, O., Teodorescu, C.M., Chauvet, O., Payen, C., Macovei, D., Turcu, R., Soran, M.L., Aldea, N., Barbu, L., 2007. Structure, morphology and magnetic properties of Fe-Au core-shell nanoparticles. Surf. Sci. 601 (18), 4352–4357. https://doi.org/10.1016/j.susc.2007.06.024.

Pandey, S., 2017. A review on constituents, pharmacological activities and medicinal uses of Glycyrrhiza Glabra. Univ. J. Pharm. Res. 2 (2), 6–11. https://doi.org/10.22270/ujpr.v2i2.rw2.

Pattanayak, M., Nayak, P.L., 2013. Green synthesis and characterization of zero valent iron nanoparticles from the leaf extract of Azadirachta indica (Neem). World J. Nano Sci. Technol. 2 (1), 6–09. https://doi.org/10.5829/idosi.wjnst.2013.2.1.21132.

Qin, Z., Li, Y., Gu, N., 2018. Progress in applications of Prussian blue nanoparticles in biomedicine. Adv. Healthcare Mater. 7 (20), 1–13. https://doi.org/10.1002/adhm.201800347.

Rao, K.J., Paria, S., 2015. Aegle marmelos leaf extract and plant surfactants mediated green synthesis of Au and Ag nanoparticles by optimizing process parameters using taguchi method. ACS Sustain. Chem. Eng. 3 (3), 483–491. https://doi.org/10.1021/acssuschemeng.5b00022.

Rizvi, S.A.A., Saleh, A.M., 2018. Applications of nanoparticle systems in drug delivery technology. Saudi Pharmac. J. 26 (1), 64–70. https://doi.org/10.1016/j.jsps.2017.10.012.

Romero, C.N., Medina, E., Vargas, J., Brenes, M., Castro, D.A., 2007. In Vitro Activity of Olive Oil Polyphenols against Helicobacter pylori. J. Agric. Food Chem. 55 (3), 680–686.

Rudakov, G.A., Tsiberkin, K.B., Ponomarev, R.S., Henner, V.K., Ziolkowska, D.A., Jasinski, J.B., Sumanasekera, G., 2019. Magnetic properties of transition metal nanoparticles enclosed in carbon nanocages. J. Magn. Magn. Mater. 472, 34–39. https://doi.org/10.1016/j.jmmm.2018.10.016.

Rudramurthy, G.R., Swamy, M.K., 2018. Potential applications of engineered nanoparticles in medicine and biology: an update. J. Biol. Inorg. Chem. 23 (8), 1185–1204. https://doi.org/10.1007/s00775-018-1600-6.

Rümenapp, C., Gleich, B., Haase, A., 2012. Magnetic nanoparticles in magnetic resonance imaging and diagnostics. Pharm. Res. 29 (5), 1165–1179. https://doi.org/10.1007/s11095-012-0711-y.

Salem, E.M., Yar, T., Bamosa, A.O., Al-Quorain, A., Mohamed, Alsulaiman, R.M., Randhawa, M.A., 2010. Comparative study of Nigella Sativa and triple therapy in eradication of Helicobacter Pylori in patients with non-ulcer dyspepsia. Sustain. Chem. Pharm. 16 (3), 207–214. https://doi.org/10.1016/j.scp.2019.100156.

Sarwar, S., Hanif, M.A., Ayub, M.A., Boakye, Y. D., Agyare, C., 2020. Fenugreek. In: Medicinal Plants of South Asia, pp. 257–271. https://doi.org/10.1016/B978-0-08-102659-5.00020-3.

Salmanroghani, H., Mirvakili, M., Baghbanian, M., Salmanroghani, R., Sanati, G., et al, 2018. Efficacy and tolerability of two quadruple regimens: bismuth, omeprazole, metronidazole with amoxicillin or tetracycline as first-line treatment for eradication of helicobacter pylori in patients with duodenal ulcer: a randomized clinical trial. PLoS ONE 13 (6), e0197096. https://doi.org/10.1371/journal.pone.0197096.

Sathiyanarayanan, G., Dineshkumar, K., Yang, Y.H., 2017. Microbial exopolysaccharide-mediated synthesis and stabilization of metal nanoparticles. Crit. Rev. Microbiol. 43 (6), 731–752. https://doi.org/10.1080/1040841X.2017.1306689.

Serhan, M., Sprowls, M., Jackemeyer, D., Long, M., Perez, I.D., Maret, W., Tao, N., Forzani, E., 2019. Total iron measurement in human serum with a smartphone. In: AIChE Annual Meeting, Conference Proceedings, 2019-Novem. https://doi.org/10.1039/x0xx00000x.

Shunmugam, R., Balusamy, S.R., Kumar, V., Menon, S., Lakshmi, T., Perumalsamy, H., 2021. Biosynthesis of gold nanoparticles using marine microbe (Vibrio alginolyticus) and its anticancer and antioxidant analysis. J. King Saud Univ. – Sci. 33 (1), 101260. https://doi.org/10.1016/j.jksus.2020.101260.

Sharma, R., Tripathi, A., 2021. Green synthesis of nanoparticles and its key applications in various sectors. Mater. Today:. Proc. https://doi.org/10.1016/j.matpr.2021.09.512.

Sharifi, A., Azizi, M., Moradi-Choghakabodi, P., Aghaei, S., Azizi, A., 2019. In vitro anti-Helicobacter pylori activity of aqueous extract from Persian Oak testa. Chin. Herbal Med. 11 (4), 394–399. https://doi.org/10.1016/j.chmed.2019.09.002.

Singera, A., Barakat, Z., Mohapatra, S., Mohapatra, S.S., 2019. Nanoscale drug-delivery systems: in vitro and in vivo characterization. Nanocarriers Drug Deliv., 395–419 https://doi.org/10.1016/B978-0-12-814033-8.00013-8.

Singh, M., Kalaivani, R., Manikandan, S., Sangeetha, N., Kumaraguru, A.K., 2013. Facile green synthesis of variable metallic gold nanoparticle using Padina gymnospora, a brown marine macroalga. Appl. Nanosci. (Switzerland) 3 (2), 145–151. https://doi.org/10.1007/s13204-012-0115-7.

Spósito, L., Oda, B.F., Vieira, J.H., Carvalho, F.L., Ramos, M., Castro, R., Crevelin, E., Crotti, A., Santos, A., Chorilli, M., Bauab, T., 2019. In vitro and in vivo anti-Helicobacter pylori activity of Casearia sylvestris leaf derivatives. J. Ethnopharmacol. 233 (April), 1–12. https://doi.org/10.1016/j.jep.2018.12.032.

Stoicov, C., Houghton, J., 2013. Green Tea and Protection against Helicobacter Infection. Tea Health Dis. Prevent., 593–601 https://doi.org/10.1016/B978-0-12-384937-3.00049-5 (Chapter 49).

Tavakoli, M., Malakooti, M.H., Paisana, H., Ohm, Y., Green Marques, D., Alhais Lopes, P., Piedade, A.P., de Almeida, A.T., Majidi, C., 2018. EGaIn-assisted room-temperature sintering of silver nanoparticles for stretchable, inkjet-printed, thin-film electronics. Adv. Mater. 30 (29), 1–7. https://doi.org/10.1002/adma.201801852.

Thakur, A.K., Raj, P., 2017. Pharmacological perspective of Glycyrrhiza glabraLinn.: a mini-review. J. Analyt. Pharmac. Res. 5 (5). https://doi.org/10.15406/japlr.2017.05.00156.

Thakkar, K.N., Mhatre, S.S., Parikh, R.Y., 2010. Biological synthesis of metallic nanoparticles. Nanomed. Nanotechnol. Biol. Med. 6 (2), 257–262. https://doi.org/10.1016/j.nano.2009.07.002.

Tombola, F., Campello, S., Luca, L.D., Ruggiero, P., Giudice, G.D., Papin, E., Zoratti, E., 2003. Plant polyphenols inhibit VacA, a toxin secreted by the gastric pathogen Helicobacter pylori. FEBS Lett. 543 (1–3), 184–189. https://doi.org/10.1016/S0014-5793(03)00443-5.

Verma, A., Dubey, J., Hegde, R.R., Rastogi, V., Pandit, J.K., 2016. Helicobacter pylori: past, current and future treatment strategies with gastroretentive drug delivery systems. J. Drug Target. 24 (10), 897–915. https://doi.org/10.3109/1061186X.2016.1171326.

Vetvicka, V., Vetvickova, J., Fernandez-Botran, R., 2016. Effects of curcumin on Helicobacter pylori infection. Annal. Transl. Med. 4 (24), 1–7. https://doi.org/10.21037/atm.2016.12.52.

Vijayan, R., Joseph, S., Mathew, B., 2018. Indigofera tinctoria leaf extract mediated green synthesis of silver and gold nanoparticles and assessment of their anticancer, antimicrobial, antioxidant and catalytic properties. Artif. Cells Nanomed. Biotechnol. 46 (4), 861–871. https://doi.org/10.1080/21691401.2017.1345930.

Wang, G., Pang, J., Hu, X., Nie, T., Lu, X., Li, X., Wang, X., Lu, Y., Yang, X., Jiang, J., Li, C., Xiong, Y.Q., You, X., 2019. Daphnetin: a novel Anti-Helicobacter pylori agent. Int. J. Mol. Sci. 20 (4). https://doi.org/10.3390/ijms20040850.

Wang, R., Liu, W.D., Wang, A.J., Xue, Y., Wu, L., Feng, J.J., 2018. A new label-free electrochemical immunosensor based on dendritic core-shell AuPd@Au nanocrystals for highly sensitive detection of prostate specific antigen. Biosens. Bioelectron. 99 (July 2017), 458–463. https://doi.org/10.1016/j.bios.2017.08.010.

Wang, L., Yang, R., Yuan, B., Liu, Y., Lin, C., 2015. The antiviral and antimicrobial activities of licorice, a widely-used Chinese herb. Acta Pharmaceutica Sinica B 5 (4), 310–315. https://doi.org/10.1016/j.apsb.2015.05.005.

Wang, L., Yang, R., Yuan, B., Liu, Y., Liu, C., 2015. The antiviral and antimicrobial activities of licorice, a widely-used Chinese herb. Acta Pharmaceutica Sinica B 5 (4), 310–315. https://doi.org/10.1016/j.apsb.2015.05.005.

Williams, L., 2011. Helicobacter pylori' infection: a review of current scientific research on the efficacy or potential of herbal medicine for the treatment of 'H. Pylori' infection of the gastric mucosa. Aust. J. Med. Herbal. 23 (3), 139–149 https://search.informit.org/doi/10.3316/informit.638770816097499.

Wittschier, N., Faller, G., Hensel, A., 2009. Aqueous extracts and polysaccharides from Liquorice roots (Glycyrrhiza glabra L.) inhibit adhesion of Helicobacter pylori to human gastric mucosa. J. Ethnopharmacol. 125 (2), 218–223. https://doi.org/10.1016/j.jep.2009.07.009.

Wu, Y., Jiang, P., Jiang, M., Wang, T.W., Guo, C.F., Xie, S.S., Wang, Z.L., 2009. The shape evolution of gold seeds and gold@silver core-shell nanostructures. Nanotechnology 20 (30). https://doi.org/10.1088/0957-4484/20/30/305602.

Yanagawa, Y., Yamamoto, Y., Hara, Y., Shimamura, T., 2003. A combination effect of epigallocatechin gallate, a major compound of green tea catechins, with antibiotics on helicobacter pylori growth in vitro. Sustain. Chem. Pharm. 47, 0244–0249. https://doi.org/10.1007/s00284-002-3956-6.

Yee, U.-K., Koo, M.-W.-L., 2001. EAnti-Helicobacter pylori activity of Chinese tea: in vitro study. Aliment. Pharmacol. Ther. 14 (5), 635–638. https://doi.org/10.1046/j.1365-2036.2000.00747.x.

Zaleska-Medynska, A., Marchelek, M., Diak, M., Grabowska, E., 2016. Noble metal-based bimetallic nanoparticles: the effect of the structure on the optical, catalytic and photocatalytic properties. Adv. Colloid Interface Sci. 229, 80–107. https://doi.org/10.1016/j.cis.2015.12.008.

Zare, Y., Rhee, Y.K., Hui, D., 2017. Influences of nanoparticles aggregation/agglomeration on the interfacial/interphase and tensile properties of nanocomposites. Compos. B Eng. 122, 41–46. https://doi.org/10.1016/j.compositesb.2017.04.008.

Zamani, M., Ebrahimtabar, F., Zamani, V., Miller, W.H., Alizadeh-Navaei, R., Shokri-Shirvani, J., Derakhshan, M.H., 2018. Systematic review with meta-analysis: the worldwide prevalence of Helicobacter pylori infection. Aliment. Pharmacol. Ther. 47 (7), 868–876. https://doi.org/10.1111/apt.14561.

Zhang, J., Post, M., Veres, T., Jakubek, Z.J., Guan, J., Wang, D., Simard, B., 2006. Laser-assisted synthesis of superparamagnetic Fe@Au core−shell nanoparticles. J. Phys. Chem. B 110 (14), 7122–7128. https://doi.org/10.1021/jp0560967.

Zhu, S., Zhu, L., Yu, J., Wang, Y., Peng, B., 2019. Anti-osteoclastogenic effect of epigallocatechin gallate-functionalized gold nanoparticles in vitro and in vivo. Int. J. Nanomed. 14, 5017–5032. https://doi.org/10.2147/IJN.S204628.